Identification and Characterization of Substrates for the *Arabidopsis thaliana* RING-Type E3 Ligases XBAT32 and KEG

by

Victoria Sullivan

Submitted in partial fulfillment of the
requirements for the degree of Master of Science

at

Dalhousie University
Halifax, Nova Scotia
July 2016

I dedicate this work to Jordan, with great appreciation for your continuous support.

TABLE OF CONTENTS

LIST OF TABLES

LIST OF FIGURES

ABSTRACT

The ubiquitin proteasome system (UPS) challenges transcription as the primary regulatory mechanism in the plant kingdom, influencing many cellular processes by selectively degrading proteins. E3 ubiquitin ligases are the UPS elements responsible for endowing the UPS pathway with specificity, by selecting substrates to be targeted to the 26S proteasome for degradation. Many E3 ubiquitin ligases have critical functions related to plant hormone perception, signaling and response. Arabidopsis Keep on Going (KEG) and XB3 ortholog 2 in *Arabidopsis thaliana* (XBAT32) are E3 ubiquitin ligases intimately related to the hormones abscisic acid (ABA) and ethylene, respectively. I investigated the relationship between each of these E3 ligases and their substrates. Calcineurin B-like Interacting Protein Kinase 26 (CIPK26) is a substrate of KEG and the UPS, while N-MYC DOWNREGULATED-LIKE 1 (NDL1) is potentially a substrate of XBAT32. I further characterized the relationship between CIPK26, KEG and ABA using transgenic plant lines in a variety of assays, including cell free degradation assays and cycloheximide (CHX) chase assays. I demonstrated that activated CIPK26 promotes KEG degradation and showed that CIPK26 overexpression increases KEG turnover in the presence of ABA. This research supports a model where, in the presence of ABA, CIPK26 phosphorylates KEG in order to negatively regulate its' activity and promote its degradation. Further, I provide evidence to support a role for XBAT32 and the UPS in regulating NDL1 stability, through the use of cell free degradation assays, a semi-*in vitro* ubiquitination assay, and a pull down assay. I offer support for an interaction between NDL1 and XBAT32, demonstrate that NDL1 is ubiquitinated and degraded by the 26S proteasome, and show that XBAT32 is likely to be required for this degradation. These findings broaden our understanding of the roles of XBAT32 related to lateral root development. Through this work we obtain a more complete understanding of the ways in which the UPS interacts with crucial plant hormones implicated in growth, development, and environmental stress response. This knowledge could contribute to the development of plants with a capacity to grow and thrive under adverse environmental conditions, of importance because climate change is having a major impact on crop viability and soil health.

LIST OF ABBREVIATIONS USED

A. thaliana	*Arabidopsis thaliana*
ABA	Abscisic Acid
ABF1	Abscisic Acid Responsive Element-Binding Factor 1
ABF3	Abscisic Acid Responsive Element-Binding Factor 3
ABI1	Abscisic Acid Insensitive 1
ABI2	Abscisic Acid Insensitive 2
ABI5	Abscisic Acid Insensitive 5
ABRC	Arabidopsis Biological Resource Center
ABRE	Abscisic Acid Responsive Element
ACC	1-aminocyclopropane-1-carboxylic acid
ACS	1-aminocyclopropane-1-carboxylic acid synthase
ADP	Adenosine diphosphate
AGB1/AGG2	Arabidopsis G-protein beta subunit 1/G-protein gamma subunit 2
ATP	Adenosine triphosphate
BRCT	Breast Cancer 1, early onset C Terminus
bZIP	Basic leucine zipper
C-terminus	carboxyl-terminus
CBL	Calcineurin B-like
cDNA	Complementary deoxyribonucleic acid
CHX	Cycloheximide
CHYR1	An E3 ubiquitin ligase
CIPK	Calcineurin B-like Interacting Protein Kinase
CIPK26	Calcineurin B-like Interacting Protein Kinase 26

$CIPK26^{KR}$	Inactive calcineurin B-like interacting protein kinase
$CIPK26^{TD}$	Constitutively active calcineurin B-like interacting protein kinase 26
Col-0	Columbia ecotype
CP	Core particle
DTT	DL-Dithiothreitol
DUBs	Deubiquitinating enzymes
ECL	Enhanced Chemiluminescence
EDTA	Ethylenediaminetetraacetic acid
FDH	Formate dehydrogenase
GST	Glutathione S-transferase
GUS	β-glucuronidase
h	Hour
HA	Hemagglutinin
HECT	Homologous to E6-associated protein carboxyl-terminus
HERC	Homologous to E6-associated protein carboxyl-terminus and RCC-1
HERC2	RCC-1 like 2
His	Histidine
Ile	Isoleucine
IPTG	isopropyl-β-D-thiogalactopyranoside
JA	Jasmonic acid
kDa	kiloDaltons
KEG	Keep on Going

mg	Milligram
MG132	N-(benzyloxycarbonyl)leucinylleucinylleucinal Z-Leu-Leu-Leu-al
min	Minute
mM	Millimolar
MS	Murashige and Skoog
N-terminus	amino-terminus
NDL	N-MYC DOWNREGULATED LIKE
NDL1	N-MYC DOWNREGULATED LIKE-1
NDR	N-myc Downregulated
NDRG	N-MYC DOWNREGULATED GENE
ng	Nanogram
OD	Optical density
PAGE	Polyacrylamide gel electrophoresis
PBS	Phosphate-buffered saline
PMSF	Phenylmethylsulfonyl fluoride
PP2C	Clade A type 2C protein phosphatases
PVDF	Polyvinylidene fluoride
RCC-1	Regulator of chromosome condensation 1
RING	Really Interesting New Gene
RP	Regulatory particle
RPM	Revolutions per minute
RT	Room temperature
SAM	S-adenosylmethionine
SCF	Skp1-Cullin-F-box

SDS	sodium dodecyl sulfate
SE	Standard error
Skp1	S-phase kinase-associated protein 1
SNF	Sucrose non-fermenting
SnRK	Sucrose non-fermenting-related kinase
SUMO	Small Ubiquitin-like Modifier
TBS	Tris-buffered saline
TBS-T	Tris-buffered saline-Tween 20
UBA	Ubiquitin-activating enzyme
UBP	Ubiquitin-associated protein domain
UBC	Ubiquitin-conjugating enzyme
UBD	Ubiquitin-binding domains
UPS	Ubiquitin Proteasome System
V	Volts
WB	Western blot
WD40	Tryptophan-aspartic acid (Beta-transducin)
wt	Wild type
XB3	XA21-binding protein 3
XBAT	XB3 ortholog in *Arabidopsis thaliana*
XBAT32	XB3 ortholog 2 in *Arabidopsis thaliana*
Y2H	Yeast two-hybrid
YFP	Yellow fluorescent protein

ACKNOWLEDGEMENTS

I thank Dr. Sophia Stone for her guidance and support throughout the course of this project. Your commitment to the success of your students is extraordinary.

To my committee, Dr. Thomas MacRae and Dr. Patrice Côté, your support and wisdom have been invaluable.

To my lab-mates, Daryl McNeilly, Sarah McVey, Dalal Alatoubi, and Nathieli Schiavi; thank you for acting as my support system on a daily basis. You made long days much more bearable and taught me so much.

To Dr. Wendy Lyzenga and Dr. Hongxia Liu, former Stone lab members and my current collaborators; thank you for your guidance on techniques, protocols, and presentation of data.

Ashar Gaskin, an undergraduate student in our lab, provided assistance with ABA-sensitivity assays and conducted a second trial independently. Sam Campbell, an honors student, conducted analysis on CIPK26 activation state, with my guidance.

I thank Jordan, who accompanied me to the lab late at night and on the weekends, and listened to me talk endlessly about E3 ligases and protein bands. Your support and unwavering confidence in me kept me going. To my family, thank you for your ongoing love and support.

CHAPTER 1: INTRODUCTION

1.1 The Ubiquitin Proteasome System (UPS)

The ubiquitin proteasome system (UPS) represents a complex and critical route for the regulated removal of specific proteins in eukaryotic cells; it is highly conserved and essential for normal development and functioning of all eukaryotic organisms (Smalle & Vierstra, 2004). The UPS is the primary ATP-dependent protein degradation pathway in eukaryotic cells, operating in the cytosol and the nucleus (Bhattacharyya et al., 2014). It consists of two distinct, sequential steps; first, a target substrate is selected and ubiquitinated, followed by breakdown of the modified substrate by the 26S proteasome, a protease complex. Proteins regulated by the UPS are modified with a minimum of four ubiquitin moieties, which form a polyubiquitin chain signalling delivery to the proteasome (Thrower et al., 2000).

The UPS regulates a myriad of critical enzymes, regulatory and structural proteins (Stone, 2014). The UPS is a system with essential roles in plant growth, development, and adaptation to external environmental conditions, including abiotic and biotic stresses (Stone & Callis, 2007; Smalle & Vierstra, 2004). The UPS is a central modulator of chromatin structure, epigenetics, homeostasis and cell cycle progression (Komander & Rape, 2012; Craig et al., 2009; Smalle & Vierstra, 2004). In *Arabidopsis thaliana*, a significant portion of the genome, nearly 6%, encodes for UPS components (Smalle & Vierstra, 2004; Hua & Vierstra, 2011). Mutations in the ubiquitin proteasome system in *Arabidopsis* result in impeded development, altered photomorphogenesis and circadian rhythms, susceptibility to pathogen invasion, and disrupted hormone responses (Craig et al., 2009).

1.1.1 Ubiquitination

Ubiquitin is linked to nearly every facet of plant biology and the UPS rivals transcription as the dominant regulatory mechanism in plants (Vierstra, 2009). Ubiquitination, a post-translational modification, is the process whereby globular ubiquitin molecules of 76 amino acids, 8.5 kiloDaltons (kDa), become attached to substrates, in order to modify their function (Jentsch & Pyrowolakis, 2000). Eukaryotic cells employ ubiquitin as a regulatory molecule, with ubiquitin acting as a covalent modifier of other proteins, as well as itself (Callis, 2014). The nearly invariant nature of ubiquitin from yeast to plants to humans, as well as its' expression in every tissue type, is suggestive of strong evolutionary pressure for conservation of the ubiquitin structure (Komander & Rape, 2012). Numerous and diverse cellular proteins become modified by ubiquitin and often the modified substrates are essential intracellular signaling pathway elements (Weissman et al., 2011; Callis, 2014). The covalent attachment of ubiquitin to selected substrates enables changes in activity, trafficking, localization and abundance/longevity (Stone, 2014). Functions of ubiquitin include the regulation of signaling pathways and the modulation of metabolic pathways (Vierstra, 2009). Ubiquitin even influences gene expression by way of histone modifications and the modulation of transcription factor activity and abundance (Callis, 2014).

Ubiquitination is a sequential and multistep process, requiring the activity of three enzymes: E1, ubiquitin-activating enzyme (UBA), E2, ubiquitin-conjugating enzyme (UBC), and the E3 ubiquitin ligase (Smalle & Vierstra, 2004; Stone, 2014) (Fig. 1). The attachment of ubiquitin to a substrate commences with ATP-dependent ubiquitin activation by E1, generating a high-energy thioester-linked intermediate (Ciechanover et al., 1980). Ubiquitin is then transferred to E2, which forms an E2-ubiquitin intermediate,

again connected through a thioester linkage. The transfer of ubiquitin onto a substrate occurs when the target-recruiting E3 ubiquitin ligase interacts with the E2-ubiquitin intermediate. The E3 endows the pathway with specificity by selecting the target protein and mediating conjugation of ubiquitin to an internal lysine residue of the substrate (Vierstra, 2009; Sun & Chen, 2004) (Fig. 1). The importance of E3 enzymes is reflected by their great abundance and diversity across species (Weissman et al., 2011). The Arabidopsis genome is thought to encode over 1300 E3s, or components of E3 complexes (Kraft et al., 2005; Stone et al., 2005; Hua & Vierstra, 2011). Once an initial ubiquitin molecule is attached to a substrate, a chain of ubiquitin molecules can be generated (Komander & Rape, 2012).

Ubiquitin moieties are covalently bound to selected substrates through lysine residues, however, there is a great deal of variability in the ways in which ubiquitin attaches (Glickman & Ciechanover, 2002). A single ubiquitin moiety may attach to one (monoubiquitination), or to numerous (multimonoubiquitination) lysine residues of a target protein. There also exists the possibility of attachment of multiple (polyubiquitination) ubiquitin molecules as a chain onto a specified lysine residue of a selected substrate. The initiation site for ubiquitin linkage to the lysine residue of a substrate is the carboxyl group of ubiquitin's crucial glycine residue, situated at the end of its six-residue carboxyl-terminus (Craig et al., 2009). With polyubiquitination, the initial ubiquitin acts as an 'acceptor' for subsequently added ubiquitins (Behrends & Harper, 2011). Seven lysine residues in the amino-terminus of ubiquitin are the key to ubiquitin chain assembly (Komander & Rape, 2012). Each lysine residue forms ubiquitin-ubiquitin linkages, which contribute to the architectural diversity of polyubiquitin chains (Nakasone et al., 2013). Polyubiquitin chains can be either homogenous using the same lysine

Figure 1. The Ubiquitin Proteasome System. E1 (ubiquitin-activating enzyme) activates ubiquitin in an ATP-dependent manner and the ubiquitin molecule is next transferred to the E2 (ubiquitin-conjugating enzyme). The E2-ubiquitin intermediate interacts with the E3 ubiquitin ligase, the element responsible for endowing the pathway with specificity. The ubiquitin moiety is transferred from the E2-ubiquitin intermediate to a lysine residue of the target substrate bound to the E3. This multi-step process repeats to form a polyubiquitin chain. Following chain formation, the target substrate is degraded via the 26S proteasome, a large multi-subunit protease complex.

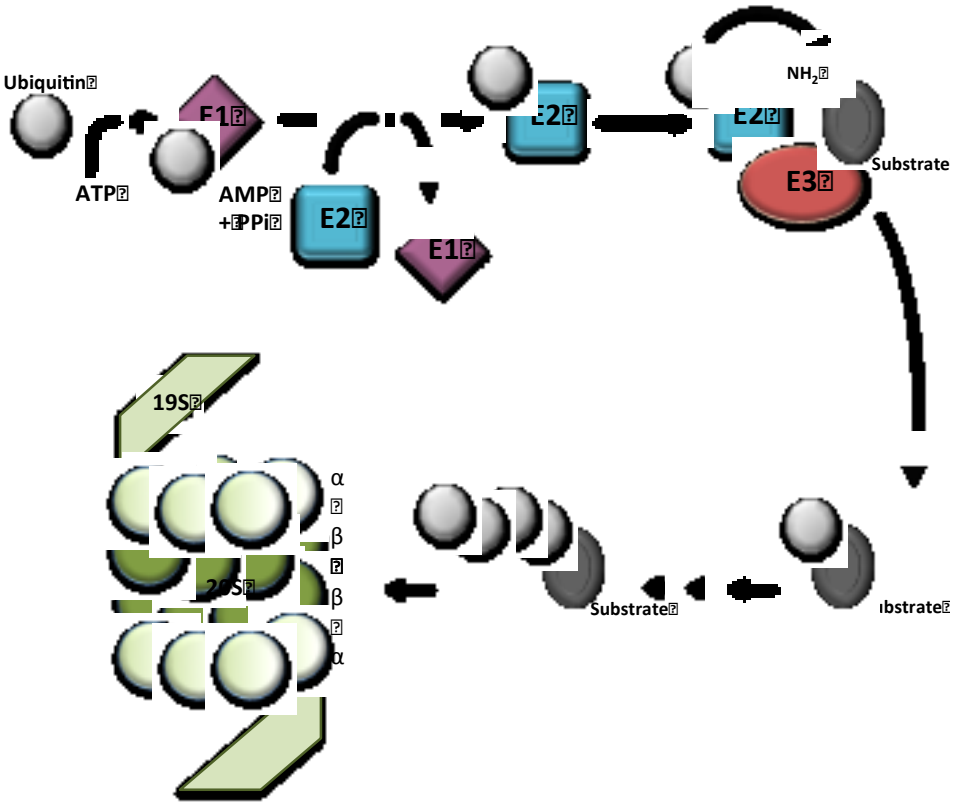

26S Proteasome

residue to form a chain, or heterogeneous using a mix of lysine residues to form ubiquitin-ubiquitin linkages (Li & Ye, 2008). Ubiquitin chains have 'compact' conformations, in which interaction occurs between adjacent moieties, and 'open' conformations, in which there are no interfaces extant, with the exception of the specific linkage site (Komander & Rape, 2012). These conformations affect how binding partners recognize ubiquitin chains. It is possible for ubiquitin chain editing to occur, where one chain type is replaced by a chain of differing topology, often resulting in an altered fate for the modified substrate. How editing unfolds has not been fully characterized (Komander & Rape, 2012).

Adding an additional layer of intricacy, ubiquitination is reversible (Liu et al., 2005). Reversibility is attributed to deubiquitinating enzymes (DUBs), which cleave ubiquitin from modified substrates (Turcu et al., 2009). DUBs are multifunctional enzymes that modify chains of varying length, linkage type and topology (Komander & Rape, 2012; Turcu et al., 2009). DUBs serve critical roles, such as the prevention of constitutively active ubiquitination. Some DUBs disassemble chains regardless of linkage type while others demonstrate specificity (Komander & Rape, 2012). The regulation of ubiquitination is thus precise, and controlled in such a way as to specify particular, distinct, fates to ubiquitinated proteins.

1.1.2 Outcomes of Ubiquitination

Ubiquitination represents an adaptable and versatile means to regulate protein function; attachment of one or more ubiquitin moieties onto a protein target results in many possible outcomes for the modified substrate. The outcomes depend on the protein target, the number of ubiquitin moieties bound to the target, the location of ubiquitin

attachment, as well as the ability of binding partners to differentiate between ubiquitin modification types (Callis, 2014). Once a protein has received a specific ubiquitin tag, linkage specific effector proteins possessing ubiquitin-binding domains (UBDs) interpret the meaning of the modification and modulate precise outcomes (Grabbe & Dikic, 2009). The flexibility of the ubiquitination system allows for a plethora of potential outcomes (Bremm et al., 2010; Behrends & Harper, 2011; Callis, 2014).

The most common and best-characterized outcome of ubiquitination is the targeting of a substrate protein for degradation via the 26S proteasome, which historically requires attachment of a lysine-48 linked polyubiquitin chain of at least four ubiquitin molecules to the target (Stone et al., 2005; Glickman & Ciechanover, 2002; Sun & Chen, 2004). The ubiquitin proteasome system mediated degradation serves critical roles during normal cellular activities by removing misfolded proteins, maintaining a pool of free amino acids, removing rate-limiting enzymes and suppressing regulatory networks (Craig et al., 2009). Multiple types of ubiquitin chains, including lysine-63 linked chains, lead to degradation (Flick et al., 2006). Moreover, proteolytic, as well as non-proteolytic fates for ubiquitinated proteins exist (Callis, 2014).

Ubiquitination controls signaling pathways through a number of processes that do not require the proteasome, much of what we know about these processes comes from animal systems (De Bie & Ciechanover, 2011; Wilkinson et al., 2005). Once ubiquitinated, some proteins trigger signal transduction cascades, others are targeted to the vacuole for degradation (Callis, 2014). Ubiquitination is linked to the recruitment of proteins to specific signaling pathways, to the initiation of a change in substrate localization, and to the regulation of substrate protein activity. For example, lysine-63 linked chains are implicated in kinase activation (Passmore & Barford, 2004). Commonly,

non-proteolytic roles for ubiquitination are the outcome of monoubiquitination, or methionine-1 and lysine-63 linked chain formation (Komander & Rape, 2012). However, lysine-48 linked ubiquitin chains are associated with consequences other than proteasomal degradation as well, including the regulation of transcription factor activity (Flick et al., 2006). Monoubiquitination is implicated in regulation of histone function, retrovirus budding, receptor endocytosis, and DNA damage repair (Hicke, 2001; Haglund et al., 2003). Monoubiquitination of lysine-63, in particular, targets substrate proteins to lysosomes (Hicke, 2001; Haglund et al., 2003; Mukhopadhyay & Riezman, 2007). Multimonoubiquitination is also involved in endocytosis of receptors (Haglund et al., 2003). It is possible for reversible ubiquitination, mediated by DUBs, to direct non-proteolytic outcomes involved in transcriptional regulation, vesicular trafficking or chromatin structure (Vierstra, 2009).

Ultimately, the joint activities of ubiquitinating, deubiquitinating and ubiquitin-binding proteins determine the outcome of ubiquitination for a modified substrate (Komander & Rape, 2012). Additional factors that affect the fate of a modified protein are protein localization and interaction with effectors (Komander & Rape, 2012). Thousands of proteins functioning in nearly every signaling pathway undergo ubiquitin modification and the potential outcomes of ubiquitination are incredibly diverse (Kim et al., 2011).

1.1.3 Ubiquitin Ligases

Ubiquitin ligases are extremely well represented in the *Arabidopsis thaliana* genome, and are the most abundant class of proteins involved in the UPS (Mazzucotelli et al., 2006). Over 1400 E3 ubiquitin ligases have been characterized in the Arabidopsis

proteome (Mazzucotelli et al., 2006). The diversity of ubiquitin E3 ligases in eukaryotic genomes contributes to the ability of the ubiquitination pathway to precisely and unambiguously modify diverse and abundant substrates.

The categorization of E3 ligases is based upon the domain type employed to interact with E2-ubiquitin intermediates (Ardley & Robinson, 2005). Three distinct groups of E3 ubiquitin ligases exist; Homologous to E6-AP Carboxyl Terminus (HECT), Really Interesting New Gene (RING), and U-box groups (Fig. 2) (Stone et al., 2005; Vierstra, 2009; Smalle & Vierstra, 2004; Mazzucotelli et al., 2006). A unique feature of the HECT group of E3 ligases is that they catalyze the formation of an isopeptide bond between a lysine residue of a target protein, and a ubiquitin molecule. This results in the generation of an E3-ubiquitin intermediate, prior to the transfer of ubiquitin to the target substrate (Verdecia et al., 2003; Stone et al., 2005). In contrast to HECT type E3s, U-box and RING-type E3s share structural similarity and function by bringing a target substrate and an E2 into close proximity in order to mediate the transfer of ubiquitin, thereby interacting non-covalently with the E2 possessing a thioester-linked ubiquitin (Verdecia et al., 2003; Smalle & Vierstra, 2004; Stone et al., 2005).

Figure 2. Mechanism of E3 ubiquitin ligase action. Schematic representation of the structure of HECT, U-box, and RING groups of E3 ubiquitin ligases. HECT E3s play a direct role in catalysis during ubiquitination, while RING and U-box E3s are scaffold/adaptor-like molecules. RING and U-box E3s bring an E2 and a substrate into close proximity to promote the transfer of ubiquitin.

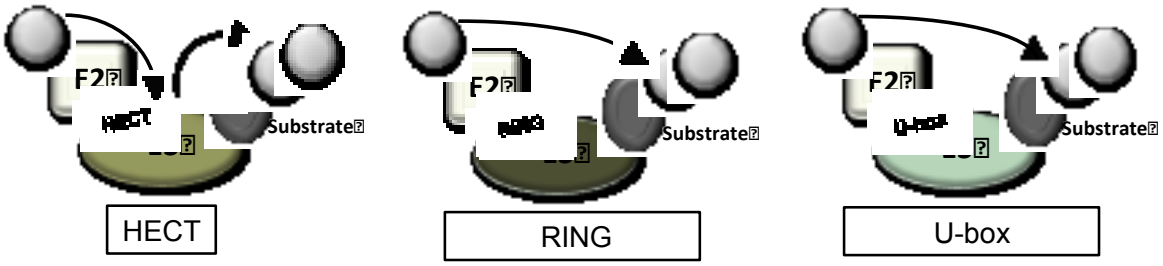
Substrate
HECT
Substrate
RING
Substrate
U-box

1.1.3.1 RING-type Ubiquitin Ligases

The Arabidopsis genome is predicted to encode 470 RING domain-containing proteins, accounting for ~2% of predicted protein-coding genes (Stone et al., 2005). RING-type E3s are characterized by a RING domain, a 70 amino acid sequence which utilizes an octet of conserved cysteine and/or histidine residues to coordinate two zinc ions (Stone et al., 2005; Freemont, 1993; Zheng et al., 2000). A characteristic cross-brace structure results from this sequence, drawing similarity to the zinc finger motif (Stone et al., 2005; Zheng et al., 2000; Borden, 2000; Pickart, 2001). The architecture of this domain is important for E2 binding and ubiquitin ligase activity (Freemont, 1993; Lorick et al., 1999). In combination with their respective E2s, RING E3 ligases initiate ubiquitin chain formation on lysines of target substrates, either in favored sequence environments of a substrate, known as chain initiation motifs, or at indiscriminate sites (Williamson et al., 2011).

RING-type E3s are classed as simple or complex (Stone et al., 2005). Included in the group of complex E3s is the anaphase-promoting complex and the multi-subunit Skp1-Cullin-F-box (SCF)-type ligase (Smalle & Vierstra, 2004). With complex E3s, which are multimeric, one protein is the substrate recognition subunit while another is responsible for recruiting the E2-ubiquitin intermediate (Stone et al., 2005; Kuroda et al., 2002; Risseeuw et al., 2003). Simple RING E3 ligases possess a substrate-binding domain and the E2-binding RING domain within a single protein; alternatively, simple E3s function in a homodimer or heterocomplex with an additional RING protein (Stone et al., 2005). RING-type ligases employ an assortment of protein interaction domains to mediate substrate binding including HERC repeat domains, a combination of Homologous to E6-AP Carboxyl Terminus (HECT) domains and RCC-1 protein domains, Ankyrin domains,

BRCT (Breast Cancer 1, early onset C Terminus) and WD40 (WD or beta-transducin) repeats (Stone et al., 2005; Garcia-Gonzalo & Rosa, 2005). Arabidopsis RING-type E3s are further categorized into 30 subgroups based on their substrate binding domains (Stone et al., 2005).

1.1.4 The 26S Proteasome

The 26S proteasome, a large 2.5 megaDalton catalytic protease complex, is implicated in most ubiquitin-mediated protein degradation and plays a pivotal role in the UPS pathway (Book et al., 2010). In plants, the 26S proteasome is disputably the principal protease (Vierstra, 2009; Book et al., 2010). With high specificity, the 26S proteasome acts via ATP hydrolysis to break down proteins including damaged, mis-folded and short-lived regulatory proteins (Bhattacharyya et al., 2014; Voges et al., 1999). Proteasomal activity is controlled in different ways including transcriptional regulation and post-translational modification (Voges et al., 1999).

The proteasome consists of approximately 33 distinct proteins, which form a tunnel-like particle consisting of a central core structure with caps on one or both sides (Voges et al., 1999; Park et al., 2010) (Fig. 1). The 26S proteasome is made up of two subparticles: a 20S core particle (CP) of ~700 kDa, consisting of 28 subunits and which possesses peptidase active sites, as well as a 19S regulatory particle (RP), which recognizes target substrates and translocates them into the core protease for subsequent degradation (Bhattacharyya et al., 2014; Finley 2009). Crystal structures reveal core particle subunits with four seven-subunit rings stacked atop one another forming a cylinder; two rings are composed of related α-subunits, and two of related β-subunits (Bhattacharyya et al., 2014; Lowe et al., 1995; Groll et al., 1997) (Fig. 1). The two β-

subunit rings are situated in the middle, while the two α-subunit rings flank the β-subunit rings on either side (Lowe et al., 1995; Groll et al., 1997), resulting in a barrel-shaped complex (Voges et al., 1999).

A ubiquitinated substrate targeted for degradation by the 26S proteasome is recognized through ubiquitin-binding proteins, or ubiquitin receptors, which traffic ubiquitinated proteins to the proteasome (Dikic et al., 2009). Proteins located in the regulatory particle of the proteasome recognize a polyubiquitinated protein and tether ubiquitinated proteins to the complex (Callis, 2014; Van Nocker et al., 1996; Fu et al., 2010). It is an isoleucine 44 (Ile44) located within a hydrophobic surface of ubiquitin that is specifically bound by the 26 proteasome (Komander & Rape, 2012). The 19s regulatory particle is responsible for protein unfolding and transporting the target protein into the proteasome core, a process that requires six ATPases within the regulatory particle (Glickman & Ciechanover, 2002; Fu et al., 2010; Lecker et al., 2006).

The protealytic activity of the 26S proteasome is mainly restricted to the 20S CP, which degrades substrate proteins (Kisselev & Goldberg, 2001). Three key proteolytic subunits are situated interiorly (Voges et al., 1999). As protein breakdown commences, the proteasome moves along the substrate, hydrolysing ATP and degrading the protein into small peptides (Bhattacharyya et al., 2014; Nussbaum et al., 1998; Kisselev et al., 1999). Proteins in the core particle complex undergo peptide bond hydrolysis at the three proteolytically active sites contained within each β-subunit ring (Callis, 2014; Eletr & Wilkinson, 2014). The three proteolytic sites on each β-ring have distinct specificities (Kisselev & Goldberg, 2001). The ‘chymotrypsin-like’ site, with its catalytic residues situated on β5 subunits, preferentially cleaves peptide bonds following a series of hydrophobic residues, the ‘trypsin-like’ site, positioned on β2 subunits, cuts following

basic amino acids, and the final site, referred to as the 'caspase-like' or 'post-acidic' site, located on β1 subunits, specifically hydrolyzes peptide bonds that follow acidic residues (Kisselev & Goldberg, 2001). Peptides generated by the proteasome vary from ~3-25 residues, with a median size of 6 residues (Lecker et al., 2006; Wenzel et al., 1994). Peptides may undergo further degradation in the cytoplasm. The ubiquitin tag on the target protein is cleaved off by deubiquitinating enzymes (DUBs) and recycled (Callis, 2014; Verma et al., 2002; Yao & Cohen, 2002).

1.2 Regulation of Hormone Signaling by UPS Components

Hormones are internal regulatory chemicals produced by organisms in order to stimulate responses by particular tissues or cells. In plants, hormones integrate internal and external signals to mediate growth, development, and cellular responses to environmental conditions. Ubiquitination regulates the synthesis, perception, and signal transduction of all major plant hormones, including abscisic acid (ABA), auxin, ethylene and jasmonic acid (JA) (Stone, 2014; Vierstra, 2009; Liu & Stone, 2013; Pauwels et al., 2015; Stone et al., 2006). At least one component of the UPS pathway acts as a central effector of responses to each of these hormones, and the UPS may have multiple control points within one signaling pathway (Vierstra, 2009). E3 ubiquitin ligases modulate plant responses to abiotic stresses including cold, drought, heat, salinity, radiation, and nutrient deprivation, and to developmental cues via effects on hormone signalling processes (Lyzenga & Stone, 2012; Yee & Goring, 2009). I focus in this thesis on two RING-type E3 ligases, XBAT32 and KEG, implicated in ethylene and ABA signaling, respectively.

1.2.1 The E3 Ligase KEG and ABA Signaling

KEG is a large single subunit E3 possessing a RING-domain and a serine/threonine (Ser/Thr) protein kinase domain as well as HERC2-like and Ankyrin repeats (Stone et al., 2006). The Ankyrin and HERC2-like repeats mediate protein-protein interactions (Liu & Stone, 2013) (Fig. 3a). Contained within the region occupied by the HERC2-like repeats is a crucial localization signal (Stone et al., 2006). KEG is implicated in pathogen resistance and the control of post-Golgi trafficking as well as the regulation and control of jasmonic acid (JA) and abscisic acid (ABA) signaling (Liu & Stone, 2013; Pauwels et al., 2015; Stone et al., 2006; Lyzenga et al., 2013; Gu & Innes, 2012; Chen et al., 2013).

Production of the phytohormone ABA increases during specific phases of plant development and in response to biotic and abiotic stress, such as drought and high salinity (Fernando & Schroeder, 2016; Weiner et al., 2010; Himmelbach et al., 2003). The abundance and activity of many ABA-responsive transcription factors must be modulated by the UPS in order to mediate alterations in gene expression that trigger the appropriate reactions to ABA, such as protective responses (Himmelbach et al., 2003; Lyzenga & Stone, 2012). KEG negatively regulates ABA signaling by reducing the abundance of basic leucine zipper (bZIP) family transcription factors, including the nucleocytoplasmic Abscisic Acid Insensitive 5 (ABI5), Abscisic Acid Responsive Element-Binding (ABRE-binding) Factor 3 (ABF3), and ABF1 (Liu & Stone, 2013; Stone et al., 2006; Chen et al., 2013). KEG ubiquitinates these elements, targeting them for degradation by the 26S proteasome (Chen et al., 2013). *Arabidopsis thaliana* KEG mutant (*keg-1*) seedlings undergo growth arrest following germination, however, when either *ABI5*, *ABF3*, or *ABF1* is knocked-out in *keg-1*, this characteristic early growth arrest phenotype can be

partially rescued. The double knockouts display slightly improved growth, as well as the emergence of the first set of true leaves, a phenotype not apparent in *keg-1* seedlings (Chen et al., 2013). This partial rescue suggests deregulated ABA signaling is a factor in the severity of the KEG mutant phenotype (Stone et al., 2006; Chen et al., 2013).

KEG has a complex regulatory relationship with ABI5, which promotes growth arrest early in seedling development in response to stressful environmental conditions (Lopez-Molina et al., 2001; Stone, 2014). When growth conditions are favourable, and ABA levels are low, KEG targets ABI5 for degradation, thereby preventing the initiation of ABA responses, and ensuring normal seedling establishment (Liu & Stone, 2010; Stone, 2014; Stone et al., 2006; Lyzenga et al., 2013). Increased ABA levels result in ABI5 accumulation, as well as inhibited ABF1 and ABF3 degradation (Chen et al., 2013). The accumulation of ABI5 in the presence of ABA involves KEG self-ubiquitination and degradation via the 26S proteasome (Liu & Stone, 2010). KEG self-regulation in the presence of ABA is phosphorylation dependent (Liu & Stone, 2010). Until recently, the upstream signaling events responsible for stimulating this phosphorylation and ABA-mediated self-ubiquitination and degradation had not been elucidated.

1.2.1.1 KEG Regulation of CIPK26

KEG is involved in the ubiquitin-dependent degradation of Calcineurin B-like Interacting Protein Kinase 26 (CIPK26), a member of the CBL-Interacting Protein Kinase (CIPK) family (Lyzenga et al., 2013). KEG interacts with and targets CIPK26 for degradation by the 26S proteasome when ABA levels are low (Lyzenga et al., 2013).

CIPK26 is a member of a family of serine/threonine protein kinases known as CIPKs, or Sucrose Non-Fermenting (SNF)-related Kinase (SnRK) 3. CIPK/SnRK3s belongs to a group of SNF1-related kinases including the SnRK1 and SnRK2 subfamilies (Hrabak et al., 2003). CIPKs interact with Calcineurin B-like (CBL) proteins and clade A type 2C protein phosphatases (PP2Cs) (Weinl & Kudla, 2009; Lee et al., 2007; Ohta et al., 2003). CBLs compose a key family of calcium sensing proteins, which form CBL-CIPK complexes. CIPK self-inhibition releases upon CBL binding (Weinl & Kudla, 2009). For CIPKs to achieve full activation, they must be phosphorylated on their activation loop, and they must interact with phosphorylated CBL proteins (Hashimoto et al., 2012; Chaves-Sanjuan et al., 2014). The CBL-CIPK complexes regulate ion homeostasis and fluxes via ion transporters and by relaying responses to environmental signals in plants (Hashimoto et al., 2012; Yu et al., 2014).

CIPK26 is an ABA-related kinase that positively regulates ABA signaling and abiotic stress response (Lyzenga et al., 2013; Yu et al., 2014). CIPK26 interacts with two PP2Cs that are core ABA-signaling components; abscisic acid insensitive (ABI) 1, and ABI2 (Lyzenga et al., 2013; Lan et al., 2011). This CIPK26 and ABI1 or ABI2 interaction may function as a kinase-phosphatase pair regulating ABA signal transduction (Lyzenga et al., 2013; Lan et al., 2011). Moreover, CIPK26 phosphorylates ABI5 (Lyzenga et al., 2013). When CIPK26 is overexpressed in *Arabidopsis thaliana* seedlings, the plants become hypersensitive to the inhibitory effects of ABA, further linking CIPK26 to ABA signaling (Lyzenga et al., 2013). The link between ABA, CIPK26 and KEG suggests that in order to suppress ABA signaling during development, and to guarantee proper early seedling establishment, KEG must target the kinase CIPK26 and downstream transcription factors, such as ABI5, for degradation (Fig. 3b).

Figure 3. Relationship between KEG, ABA signaling and CIPK26. a) KEG consists of a Really Interesting New Gene (RING) domain, a Ser/Thr protein kinase domain, 9 Ankyrin repeats and 12 RCC-1-like 2 (HERC2-like) repeats. (Modified from Stone et al., 2006.) b) When ABA is absent or low, in favourable growth conditions, KEG negatively regulates the ABA pathway by targeting ABA-responsive TFs, including ABI5, ABF1, and ABF3, and CIPK26 for degradation by the 26S proteasome. CIPK26 is simultaneously negatively regulated by PP2Cs. When ABA is present during stress PP2Cs are inhibited, CIPK26 is phosphorylated and it is thought to phosphorylate and stabilize ABA-responsive transcription factors. Phosphorylation inhibits KEG activity and stability because it leads to self-ubiquitination for subsequent degradation. ABA-responsive transcription factors are thus not targeted for degradation by KEG, ABI5 accumulates and ABF1 and ABF3 are stabilized and modulate an appropriate ABA-response.

a

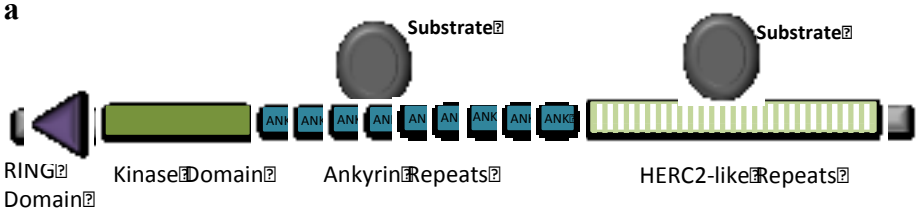
Substrate
Substrate
RING Domain
Kinase Domain
Ankyrin Repeats
HERC2-like Repeats

b

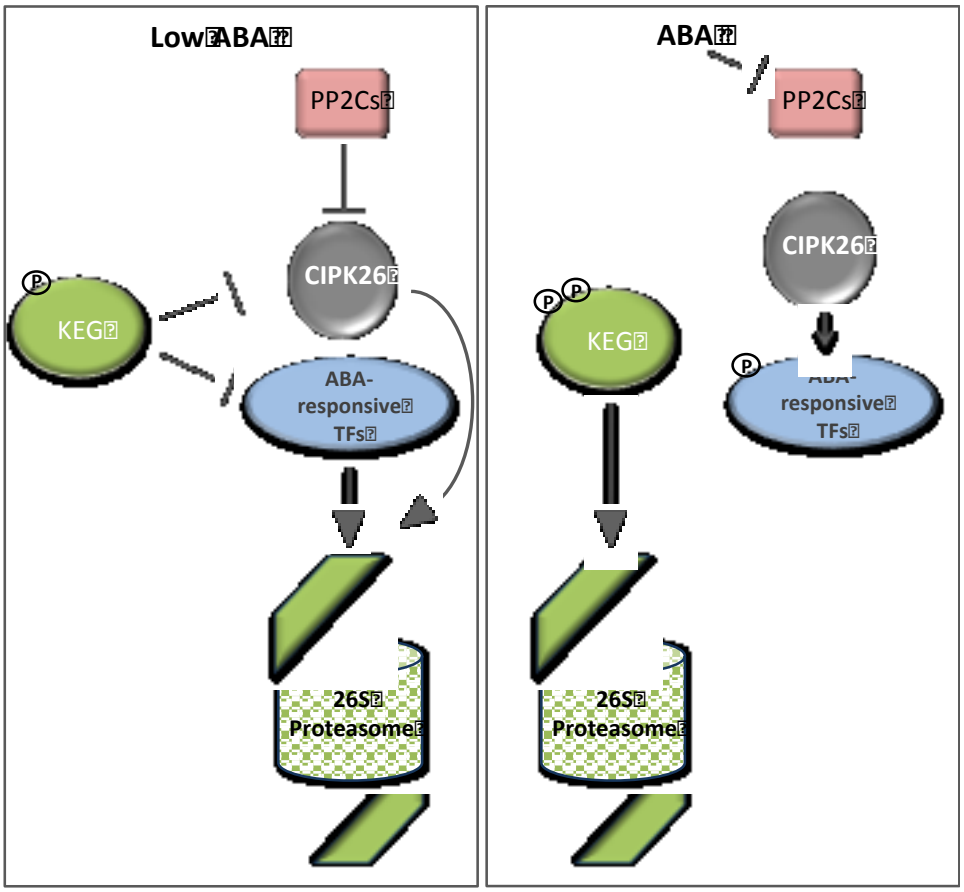
Low ABA
PP2Cs
CIPK26
KEG
ABA-responsive TFs
26S Proteasome
ABA
PP2Cs
CIPK26
KEG
responsive TFs
26S Proteasome

1.2.2 XBAT32 and Ethylene

XB3 ortholog 2 in *Arabidopsis thaliana* (XBAT32) is a monomeric RING-type E3 ligase involved in plant hormone signaling (Lyzenga & Stone, 2012). XBAT32 is one of five *Arabidopsis* proteins structurally related to *Oryza sativa* (rice) protein XB3 (Nodzon et al., 2004; Stone et al., 2006; Wang et al., 2006). It is a core member of the RING domain-containing ankyrin (RING-ankyrin) E3 ligase sub-group, along with XBAT31, XBAT33, XBAT34, XBAT35 and XBAT36 (Stone et al., 2006; Kraft et al., 2005; Wang et al., 2006; Sedgwick & Smerdon, 1999). XBAT32 contains Ankyrin repeat domains at its N-terminal half, as well as a RING finger motif (Fig. 4a). XBAT32 is thought to localize to cellular membranes (Nodzon et al., 2004).

XBAT32 is involved in ethylene homeostasis (Lyzenga et al., 2012), a critical plant hormone implicated in growth and stress. During normal plant development, biosynthesis of ethylene is tightly regulated at low levels, however; in particular developmental stages, such as germination, or in response to environmental conditions, such as hypoxia, ethylene production increases to facilitate physiological change (Lyzenga & Stone, 2012; Wang et al., 2002). A link between XBAT32 and ethylene was initially hypothesized when it was noted that the loss of XBAT32 in *Arabidopsis* yields ethylene-associated phenotypes, including a mild triple response in dark-grown seedlings, decreased plant height, and production of very few to no lateral roots by *xbat32-1* seedlings (Prasad et al., 2010). The reduced lateral root phenotype resulted from significant ethylene overproduction in these seedlings (Prasad et al., 2010). XBAT32 maintains appropriate ethylene levels by controlling the abundance and degradation of the 1-aminocyclopropane-1-carboxylic acid (ACC) synthases (ACSs) ACS4 and ACS7, enzymes that mediate conversion of S-adenosylmethionine (SAM) to the ethylene

precursor ACC, the rate-limiting step of ethylene biosynthesis (Fig. 4b) (Lyzenga et al., 2012; Yang & Hoffman, 1984; Wang et al., 2002).

While XBAT32 negatively regulates ethylene biosynthesis, ethylene, in turn, negatively regulates lateral root development through a mechanism involving auxin (Negi et al., 2008), a hormone that controls plant growth and development in response to several intrinsic and extrinsic signals, including environmental and developmental cues. During *Arabidopsis* development auxin gradient formation is critical for the establishment of all plant organs (Santos et al., 2010; Negi et al., 2008). Localized auxin accumulation promotes the initiation of root branching, and ultimately lateral root development, by stimulating activation of a quiescent pericycle cell (De Smet et al., 2007; Dubrovsky et al., 2008). The differentiated pericycle cell undergoes consecutive, coordinated divisions that produce a lateral root primordium and subsequently a lateral root (Malamy & Benfey, 1997; Casimiro et al., 2001). Auxin synthesis, transport, and signaling are pivotal to all stages of lateral root development (Prasad et al., 2010). Ethylene suppresses lateral root formation by inhibiting localized auxin accumulation (Prasad et al., 2010; Negi et al., 2008). XBAT32 is therefore required for lateral root initiation promoted by auxin and auxin partially rescues the reduced lateral root phenotype of *xbat32-1* plants (Nodzon et al., 2004).

1.2.2.1 XBAT32 Regulation of N-MYC DOWNREGULATED LIKE-1 (NDL1)

N-MYC DOWNREGULATED LIKE-1 (NDL1) is a novel proposed target of XBAT32 implicated in the formation and modulation of auxin gradients (Klopffleisch et al., 2011; Mudgil et al., 2013). A yeast-two hybrid (Y2H) screen identified NDL1 as a

potential interactor of XBAT32 (Klopffleisch et al., 2011), suggesting, because XBAT32 is an E3 ligase, that NDL1 may turnover in a UPS dependent manner.

NDL1 is one of three members of the *Arabidopsis* family of N-MYC DOWNREGULATED-LIKE (NDL) proteins, named for their likeness to mammalian N-myc Downregulated (NDR) proteins (Mudgil et al., 2009). NDL proteins are members of the alpha/beta hydrolase superfamily, containing a characteristic alpha/beta hydrolase fold, a NDR domain, a conserved patch of 23 hydrophobic amino acids, and a conserved aspartic acid (Mudgil et al., 2009; Khatri & Mudgil, 2015). NDL proteins were initially described in sunflower (sunflower-21 (SF21)) and were characterized as cell specific proteins in stigmatic and transmitting tissue, before being classified as a family of signaling elements in pollen-pistil interaction (Khatri & Mudgil, 2015; Kräuter-Canham et al., 1997; Lazarescu et al., 2006).

In *Arabidopsis,* NDL proteins were first identified in a screen for ligands of the Arabidopsis G-protein beta subunit/G-protein gamma subunit 2 (AGB1/AGG2) dimer of the heterotrimeric G-protein complex (Mudgil et al., 2009; Zhou et al., 2001). Because NDL proteins interact with the heterotrimeric G-protein complex, they are considered effectors of G-protein signaling with central functions in root and shoot development (Mudgil et al., 2009, 2013; Khatri & Mudgil, 2015). NDL proteins regulate lateral root formation through signaling pathways, modulating root auxin transport, gradients and steady-state levels of mRNA encoding for two auxin transport facilitators (Mudgil et al., 2009; Mudgil et al., 2013). When *NDL* family gene expression is reduced, and when *NDL1* is overexpressed, auxin transport and auxin maxima are affected, as is overall root architecture (Mudgil et al., 2009). The auxin-NDL1 signaling mechanism also possesses feedback loops; auxin treatment is thought to negatively regulate NDL1 (Mudgil et al.,

2009).

A novel ABA-related role is proposed for NDL family proteins in plant abiotic stress responses by regulating microtubule organization (Khatri & Mudgil, 2015). This proposal is based upon similarity of NDL1 with animal N-MYC DOWNREGULATED GENE (NDRG) and shared interactive ligands, suggestive of related functions (Khatri & Mudgil, 2015). NDRG is a microtubule-associated protein that facilitates microtubule organization, through acetylation and effects on α-tubulin stability (Khatri & Mudgil, 2015). Under abiotic stress in plants, microtubule depolymerisation and reorganization are thought to be crucial for tolerance and survival, and ABA is involved in microtubule reorganization (Sakiyama and Shibaoka, 1990; Shibaoka, 1994; Khatri & Mudgil, 2015). The details of this potential function for NDL proteins remain unclear, however, the fundamental nature of the other roles played by NDL proteins suggests their activity must be carefully regulated, perhaps in part by XBAT32 (Fig. 5).

Figure 4. XBAT32 structure and regulation of ethylene biosynthesis. a) XBAT32 consists of a series of amino-terminal Ankyrin repeats (ANK) and a RING domain. (Structure adapted from Yuan et al., 2013.) b) XBAT32 maintains appropriate ethylene biosynthesis by negatively regulating 1-aminocyclopropane-1-carboxylate synthase 4 (ACS4) and 1-aminocyclopropane-1-carboxylate synthase 7 (ACS7), enzymes implicated in the rate-limiting step of ethylene biosynthesis. Ethylene mediates lateral root initiation by a mechanism involving auxin. Diagram from Prasad et al., 2010.

a

b

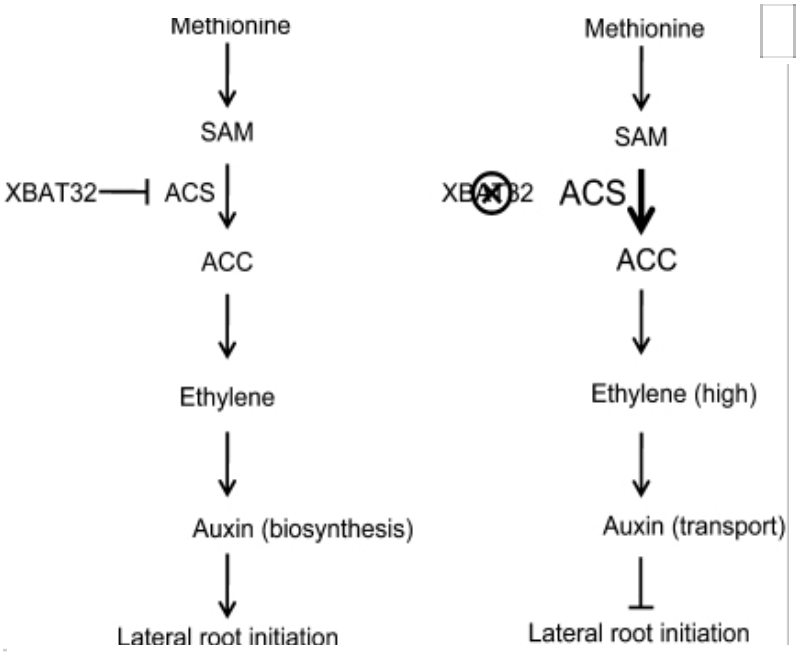

From Prasad *et al.* (2010).

Figure 5. XBAT32 and NDL1 regulate lateral root development. Solid lines show previously characterized relationships and the dotted line a suggested relationship. XBAT32 regulates ethylene biosynthesis by controlling the stability of ACSs through ubiquitination. Ethylene suppresses lateral root development via auxin. Auxin promotes lateral root development. NDL1 modulates auxin gradients. A yeast-two hybrid screen identified NDL1 and XBAT32 as potential interactors. XBAT32 may regulate NDL1 stability through ubiquitination. NDL1 and XBAT32 are mutually involved in auxin regulation, as well as lateral root formation.

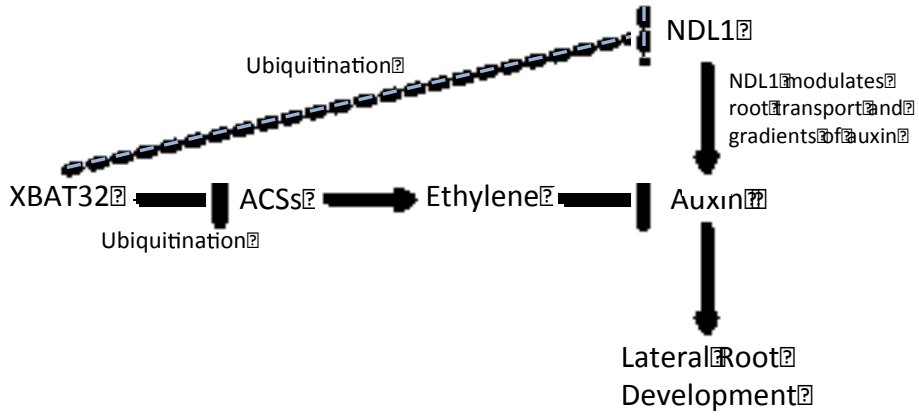
NDL1
Ubiquitination
NDL1 modulates root transport and gradients of auxin
XBAT32
ACSs
Ethylene
Auxin
Ubiquitination
Lateral Root Development

1.3 Purpose of Study

In recent years, important examples of E3 ligase and substrate pairs implicated in essential hormone signaling have been unveiled in *Arabidopsis thaliana*. However, many critical plant E3 ligase and substrate pairs remain to be uncovered; moreover, the nature and extent of relationships between E3s and target proteins remain unclear. XBAT32 and KEG are examples of such E3s. I investigated NDL1, a putative substrate of XBAT32, and further characterized the regulatory relationship between KEG and a target kinase, CIPK26. I explored whether NDL1 undergoes degradation by the UPS, investigated the role for XBAT32 in targeting NDL1 for proteasomal degradation, determined the effect of CIPK26 on KEG, and demonstrated a role for CIPK26 in ABA-induced KEG self-ubiquitination and degradation.

Enhancing our knowledge with respect to the relationships between plant E3 ligases involved in hormone signaling, and their cognate substrates broadens understanding of the subcellular processes mediating hormone signaling and responses during development and stress response. The significance of this work is in its potential utility for the cultivating of crops that develop under adverse environmental conditions, an important area for future work in order to ensure food security in a changing climate.

CHAPTER 2: MATERIALS AND METHODS

2.1 Plasmids, Cloning and Plant transformation

Previously, constructs were generated using Gateway cloning technology (Invitrogen). Full-length CIPK26 and CIPK26 kinase variants were previously described in Lyzenga et al., 2013 and KEG constructs are explained in Liu & Stone, 2010. Full length CIPK26, CIPK26^{TD}, and CIPK26^{KR} cDNA was introduced into a pEarleyGate101 Gateway plant transformation vector (Earley et al., 2006) to attain expression of C-terminal yellow fluorescent protein (YFP) and hemagglutinin (HA), under the control of the 35S cauliflower mosaic virus promoter. CIPK26^{TD} is a constitutively active version of the kinase, while CIPK26^{KR} is an inactive form of the kinase. TD signifies a mutation of a threonine residue to an aspartic acid residue and KR signifies a mutation of a lysine residue to an arginine residue. For mutagenesis of CIPK26 cDNA to CIPK26^{TD} or CIPK26^{KR}, a Phusion site-directed mutagenesis kit (Finnzymes) was employed (Gong et al., 2002*a*,*b*). Mutations were made within the activation loop of the kinase. CIPK26-YFP, CIPK26^{TD}-YFP and CIPK26^{KR}-YFP cDNAs were amplified by PCR from respective pEarleyGate101 constructs, cloned into pDONR and inserted into the 17- β-estradiol-inducible expression vector (described in Lyzenga et al., 2013) in order to generate 35S:XVE/OlexA:CIPK26-YFP-HA, 35S:XVE/OlexA:CIPK26^{TD}-YFP-HA, and 35S:XVE/OlexA:CIPK26^{KR}-YFP-HA recombinant plasmids. XBAT32 and NDL1 were respectively introduced into modified pDEST565 and pDEST527 destination vectors by Gateway cloning (Liu & Stone, 2010).

Transgenic plants were previously generated. Constructs were introduced into *Agrobacterium tumefaciens* strain GV3101 in order to generate transgenic *A. thaliana* plants by the floral dip method (Clough and Bent, 1998). For double-transgenic plants, a

35S:HA-KEG/*keg-1* line (Liu & Stone, 2010) was transformed with either *OlexA:CIPK26-YFP-HA, OlexA:CIPK26^{TD}-YFP-HA*, or *OlexA:CIPK26^{KR}-YFP-HA*. Transformed plants were selected on half-strength solid Murashige and Skoog (MS) medium supplemented with DL-phosphinothricin (Basta - Sigma-Aldrich) and kanamycin (Sigma-Aldrich). Genotyping was employed to confirm the presence of transgenes and immunoblot analysis was conducted to verify protein expression.

2.2 Plant Material and Growth Conditions

Arabidopsis thaliana ecotype Columbia (Col-0) wt and transgenic seeds were grown as described by Liu & Stone (2010). Seeds were surface-sterilized using 50% (v/v) bleach and 0.1% Triton X-100 and washed with ddH_2O. Following stratification (cold-treatment) at 4°C for 2 or 3 days, seeds germinated and were grown on solid half strength MS medium consisting of 0.8% agar and 1% sucrose, under continuous light exposure at 22°C. Plants transferred from MS medium to soil at 7-10 days were grown in a climate controlled growth chamber under photoperiodic cycles of 16 h light and 8 h dark at 22°C. For cycloheximide chase assays and cell free degradation assays, 4, 5, or 6 day-old seedlings grown under continuous light at 22°C were transferred from solid MS to liquid MS medium.

2.3 ABA Sensitivity Assay

Seeds from the transgenic *Arabidopsis thaliana* plants *35S:CIPK26-YFP-HA* and *35S:CIPK26^{TD}-YFP-HA* were sterilized and stratified at 4°C in the dark for 3 days. Seedlings were grown on solid half strength MS medium for 4 days before transfer to

solid half strength MS medium supplemented with 5μM ABA. Primary root length was monitored every 24 h through markings; thorough assessments, including ImageJ root length measurements, were made at 3 and 5 days post-transfer. Percentage inhibition of primary root elongation was determined for each transgenic line by comparing root growth in ABA treatment conditions to root growth in the absence of ABA. Assays were performed twice, with two independent replicates per trial.

2.4 Cell Free Degradation Assays

Cell free degradation assays were modified from Wang et al. (2009). Plant tissue was collected from an appropriate treatment and plant type and was homogenized in protein extraction buffer. At time zero, 10 mM $MgCl_2$ and 10 mM ATP were added to 250μg to 1mg total plant protein extract in extraction buffer and reaction mixtures were incubated at 23°C. Equal sample volumes were collected at specified time points and reactions were stopped by the addition of 5 X SDS sample loading buffer and freezing in liquid nitrogen. To ensure equal protein loading in cell free degradation assays, reaction mixtures were mixed prior to the removal of equivalent volumes of protein in extraction buffer at the indicated time intervals. Where purified recombinant protein was used in cell free degradation assays, 300ng of purified His-Flag-NDL1 protein was added to reactions at time zero. For proteasome inhibitor treatments, protein extracts were supplemented with 50 μM MG132 for 30 min prior to time zero, and addition of $MgCl_2$, ATP, and recombinant protein. For induction of CIPK26^{TD}-YFP-HA, CIPK26-YFP-HA, and CIPK26^{KR}-YFP-HA expression, 6 day-old *OlexA:CIPK26^{TD}-YFP-HA, 35S:HA-KEG/keg-1, OlexA:CIPK26-YFP-HA, 35S:HA-KEG/keg-1, and OlexA:CIPK26^{KR}-YFP-HA,*

35S:HA-KEG/keg-1 double transgenic *Arabidopsis thaliana* seedlings were treated with 20 μM 17-β-estradiol in liquid half strength MS media for 4 h prior to plant tissue collection and snap-freezing in liquid nitrogen.

2.5 Immunodetection of Proteins on Western Blots

Plant tissue was snap-frozen in liquid nitrogen and ground into a fine powder, in eppendorf tubes with a cold pestle attached to a drill, prior to resuspension in protein extraction buffer (20 mM Tris-HCl, pH 7.5, 150 mM NaCl, 1 mM EDTA, 5% glycerol, and protease inhibitor cocktail (Roche Diagnostics) or 25 mM Tris-HCl, pH 7.5, 10 mM NaCl, 10 mM $MgCl_2$, 4 mM PMSF, 5mM DTT, 10 mM ATP and protease inhibitor cocktail (Roche Diagnostics), the latter in the case of cell free degradation assays employing recombinant purified protein). Once homogenized, samples were centrifuged twice for 5 min at 17,000 g at 4°C to pellet plant debris, supernatant was transferred to a fresh tube between centrifugations, the final supernatant was recovered for use in assays or for immunoblot analysis. Cell free degradation reactions were stopped and samples were prepared for gel loading with the addition of 5 X sodium dodecyl sulfate (SDS)-PAGE sample loading buffer (0.312 M Tris-HCl, pH 6.8, 10% SDS, 25% β-mercaptoethanol, 0.05% bromophenol blue). Samples were placed in boiling water in a heating block for 3 min and centrifuged at 4,800 RPM for 3 min prior to loading on 7.5, 10, or 12.5% SDS polyacrylamide gels. Gels were run at 150 V. Depending on the assay, 25-55 μg of protein from each treatment was subject to immunoblot analysis. A semi-dry electro-transfer unit was utilized for protein transfer to polyvinylidene fluoride (PVDF) membranes (EMD Millipore). Membranes were blocked in 5% skim milk solution in

Tris-buffered saline (50 mM Tris-HCl, pH 7.5, 150 mM NaCl), 0.05% Tween 20 (TBS-T) for 1 h at room temperature (RT), followed by incubation with primary antibodies for 1 h (see Table 1). Membranes were washed for 10 min with TBS-T 3 times. Secondary antibodies were then applied for 1 h (see Table 1). Antibodies were diluted in 0.5% milk solution and used according to manufacturer's instructions (Sigma). Membranes were again washed for 10 min with TBS-T 3 times prior to visualization of protein with an Enhanced Chemiluminescence (ECL) Western Blotting Substrate kit (Thermo Scientific) and the use of Carestream Kodak film. PVDF membranes were stained with Ponceau S to visualize total protein loading.

Table 1. List of primary and secondary antibodies employed in the detection of proteins on Western blot analysis. All antibodies were obtained from Sigma-Aldrich.

Fusion Protein Tag	Primary Antibody	Dilution Factor	Secondary Antibody	Dilution Factor
Hemagglutinin (HA)	Mouse anti-HA	1:5000	anti-Mouse IgG	1:10000
Flag	Mouse anti-Flag	1:10000	anti-Mouse IgG	1:10000
Glutathione S-transferase (GST)	Rabbit anti-GST	1:10000	anti-Rabbit IgG	1:5000
Phosphate group	Rabbit anti-Phosphoserine	1:1000	anti-Rabbit IgG	1:5000

2.6 p62-Agarose Pull Down Assay

Pull down was modified from Kong et al. (2015). Wild type Arabidopsis protein extract was prepared in extraction buffer (50 mM Tris-HCl, pH 7.5, 20 mM NaCl, 1 mM PMSF, 50 μM MG132, 5 mM ATP and 10 μL protease inhibitor cocktail solution (prepared according to manufacturer's specifications from tablets (Roche Scientific)) per 1 mL extraction buffer. p62-agarose (Enzo Life Science), a ubiquitin-trap bead, was washed with two volumes of TBS-T twice. Recombinant His-Flag-NDL1 was expressed in *E. coli* strain Rosetta (DE3) and purified with Nickel-Charged Profinity IMAC Resin (Bio-Rad), as per manufacturer's specifications. 500 ng of purified recombinant His-Flag-NDL1 was added to 250 μg total Arabidopsis protein extract and they were incubated with 30 μL p62-agarose for 4 h at 4°C with shaking. Following incubation, p62-agarose was washed twice using Wash Buffer 1 (50 mM Tris-HCl, pH 7.5, 20 mM NaCl), and once using Wash Buffer 2 (50 mM Tris-HCl, pH 7.5, 220 mM NaCl). Supernatants were removed and bead samples were resuspended in 2 X SDS sample loading buffer and placed in boiling water on a heating block for 3 min. Samples were subjected to SDS-PAGE and immunoblot analysis was performed using anti-Flag antibodies to detect ubiquitinated His-Flag-NDL1 isolated by the p62-agarose.

2.7 Glutathione S-transferase (GST) Pull Down Assay

Pull down assays were performed as described (Schechtman *et al*., 2003). In brief, His-GST-XBAT32 and His-Flag-NDL1 constructs were transformed into *E. coli* strain Rosetta and grown overnight at 37°C with shaking in lysogeny broth (LB) supplemented with antibiotics. Cultures were diluted 1:50 in lysogeny broth containing antibiotic and

grown until an OD (595 nm) of approximately 0.6 was attained at which time they were induced with 0.5 mM isopropyl-β-D-thiogalactopyranoside (IPTG). Cells were pelleted and resuspended in lysis buffer (PBS, 10 uL protease inhibitor cocktail solution (prepared from tablets as per manufacturer's specifications (Roche Diagnostics)) per 1 mL lysis buffer, 1mM PMSF, 0.5% Triton X-100, 5% glycerol, 10 μL freshly prepared lysozyme solution (10 mg/ml in 10 mM Tris-HCl, pH 8.0) per 1 mL lysis buffer. Suspensions were frozen and thawed on ice twice and sonicated on ice for 1 min three times. Cell debris was pelleted and supernatants were analysed by SDS-PAGE and immunoblot analysis using anti-FLAG and anti-GST antibodies in order to optimize conditions for protein expression. Glutathione-agarose was washed twice with one volume of lysis buffer (described above). His-GST-XBAT32 and His-GST fusion protein lysates were incubated with glutathione-agarose with shaking for 2 h at 4°C. His-Flag-NDL1 fusion protein lysate was overlayed on glutathione-agarose and incubated for 2 h at 4°C. Fusion proteins were eluted from beads with 1X SDS sample loading buffer. Samples placed in boiling water in a heating block for 3 min and resolved by SDS-PAGE. Anti-Flag, anti-His and anti-GST antibodies were employed for immunoblotting to detect whether glutathione-agarose with His-GST-XBAT32 applied isolated His-Flag-NDL1.

2.8 Cycloheximide and ABA Treatment Assays

To demonstrate the effect of activated CIPK26-YFP-HA on HA-KEG protein abundance over time *in planta*, 4-day-old *OLexA:CIPK26^{TD}-YFP-HA, 35S:HA-KEG/keg-1* and *OLexA:CIPK26^{KR}-YFP-HA, 35S:HA-KEG/keg-1* double transgenic seedlings were grown for 24 h in liquid half MS medium and then exposed to either 20 μM 17-β-

estradiol dissolved in ethanol or to ethanol for 6 h. Seedlings were then treated with 500 μM cycloheximide (CHX) and tissue was collected at specified time points.

To study whether the overexpression of CIPK26-YFP-HA affects HA-KEG degradation in the presence of ABA, 4-day-old *OLexA:CIPK26-YFP-HA, 35S:HA-KEG/keg-1* seedlings were grown for 24 h in liquid MS medium and then exposed to either 20 μM 17-β-estradiol dissolved in ethanol or to ethanol for 6 h. MS medium was then replaced and supplemented with 50 μM abscisic acid (ABA) dissolved in ethanol or with ethanol and with 500 μM CHX. Tissue was then collected at the indicated time points and frozen with liquid nitrogen. Tissue samples were processed as described in Immunodetection of Proteins on Western Blot.

2.9 CIPK26 Phosphorylation Assay

Wild type Col-0, *35S:CIPK26-YFP-HA* and *35S:CIPK26^{KR}-YFP-HA* seedlings were grown on solid half strength MS media for 4 days and then transferred to liquid half strength MS media for 2 days before treatment with 100 μM ABA or with ethanol. Seedlings were collected following 30 min treatment with ABA and frozen in liquid nitrogen. Protein was extracted by grinding seedling tissue with a cold pestle and resuspending the tissue in protein extraction buffer (20mM Tris-HCl, pH 7.5, 150mM NaCl, 1mM EDTA, 1mM EGTA, 5% glycerol, protease inhibitor cocktail solution (prepared from tablets according to manufacturer's specifications (Roche Diagnostics)) containing 50 μM MG132 (Sigma). Protein concentrations were measured and equilibrated using the Bradford assay with bovine serum albumin (BSA) as the protein concentration standard. CIPK26-YFP-HA and CIPK26^{KR}-YFP-HA were isolated from

total protein extracts using anti-HA agarose affinity gel beads (Sigma) that had been washed with TBS-T twice and once with extraction buffer. Protein extract was incubated with anti-HA beads for 2.5 h at 4°C. Following centrifugation to collect the beads, beads were washed in wash buffer (20 mM Tris-HCl and 150 mM NaCl) three times and protein was eluted using SDS loading buffer. Samples were analysed by SDS-PAGE and immunoblot analysis. CIPK26-YFP-HA and CIPK26^{KR}-YFP-HA protein was detected on Western blot using anti-HA and anti-phosphoserine antibodies (Sigma-Aldrich, P3430).

2.10 Post-Translational Modification Prediction and Interaction Mapping

Ubiquitination modification site prediction was performed for Arabidopsis NDL1 with UbiProber (http://bioinfo.ncu.edu.cn/UbiProber.aspx (Chen et al., 2013)), iUbiq-Lys (http://www.jci-bioinfo.cn/iUbiq-Lys) and BDM-PUB software (http://bdmpub.biocuckoo.org/ (Li et al., 2009)). NDL1 (AT5G56750.1) sequence data were obtained from The Arabidopsis Information Resource (TAIR) database (https://www.arabidopsis.org/) and data were inserted into each software program in FASTA format. UbiProber cutoff SVM value was set at 0.5.

Experimentally determined phosphorylation site data (determined by mass spectrometry) were obtained from the PhosphAT database (http://phosphat.uni-hohenheim.de/db.html). Phosphorylation site prediction was conducted using NetPhos 2.0 (http://www.cbs.dtu.dk/services/NetPhos).

Interaction maps were generated from BioGRID (http://thebiogrid.org/). Interaction predictions are based on experimental data, including high-throughput and low-throughput yeast two-hybrid screens.

2.11 Quantitation of Protein Band Intensity

Pixel intensity analyses were conducted using ImageJ processing software (http://imagej.nih.gov/ij/) (Abramoff et al., 2004). Films used for Western blot detection were scanned and raw images were imported into ImageJ. The percentage of total protein remaining, as compared to the total protein present at time zero, was determined for each time point by measurement of the mean pixel intensity of each band with the 16-bit grey scale. Pixel intensity values were inverted in order to determine percentage of protein remaining.

CHAPTER 3: RESULTS

3.1 CIPK26 Promotes the Degradation of KEG

To determine if CIPK26 regulates KEG abundance *in planta keg-1* plant lines expressing HA-KEG (*35S:HA-KEG/keg-1*) and either CIPK26^{TD}-YFP-HA (*OlexA:CIPK26^{TD}-YFP-HA*) or CIPK26^{KR}-YFP-HA (*OlexA:CIPK26^{KR}-YFP-HA*) under the control of an estradiol inducible promoter were employed. CIPK26^{TD} is a constitutively active form of the kinase, while CIPK26^{KR} is an inactive form of the kinase. Here, cycloheximide chase assays were used to determine the effect of CIPK26^{TD} or CIPK26^{KR} on KEG abundance, providing a means to assess HA-KEG stability *in planta* in the presence and absence of a functional kinase. *OlexA:CIPK26^{TD}-YFP-HA, 35S:HA-KEG/keg-1* and *OlexA:CIPK26^{KR}-YFP-HA, 35S:HA-KEG/keg-1* seedlings were incubated with 17-β-estradiol to induce expression of CIPK26^{TD}-YFP-HA, or CIPK26^{KR}-YFP-HA, after which seedlings were treated with CHX to inhibit protein synthesis. At indicated time intervals seedlings were collected, protein extracts were prepared from the seedlings and probed with anti-HA antibodies to detect HA-KEG. HA-KEG in *OlexA:CIPK26^{TD}-YFP-HA, 35S:HA-KEG/keg-1* seedlings decreased considerably over time upon exposure to 17-β-estradiol as compared to samples taken from *OlexA:CIPK26^{TD}-YFP-HA, 35S:HA-KEG/keg-1* seedlings not exposed to 17-β-estradiol (Fig. 6a, b). Moreover, HA-KEG appeared to decline more quickly in the 17-β-estradiol treated *OlexA:CIPK26^{TD}-YFP-HA, 35S:HA-KEG/keg-1* seedlings as compared to the 17-β-estradiol treated *OlexA:CIPK26^{KR}-YFP-HA, 35S:HA-KEG/keg-1* seedlings (Fig. 6a, b). These findings indicate that CIPK26 kinase activity regulates the amount of KEG, and suggest that a constitutively active CIPK26 promotes KEG degradation *in planta*.

To test the findings described above, cell free degradation assays were performed using the same double-transgenic seedlings to evaluate HA-KEG stability in the presence of a constitutively active versus kinase inactive CIPK26 in a cell free system. *OlexA:CIPK26^{TD}-YFP-HA, 35S:HA-KEG/keg-1* and *OlexA:CIPK26^{KR}-YFP-HA, 35S:HA-KEG/keg-1* seedlings were collected following induction with 17-β-estradiol, or treatment with a solvent control. Protein was extracted and ATP and $MgCl_2$ were added to reactions at time zero. Samples were collected at indicated time points and subjected to immunoblot analysis using anti-HA antibodies. It was determined that HA-KEG levels were reduced more quickly when CIPK26^{TD}-YFP-HA was present, as compared to when CIPK26^{KR}-YFP-HA, the inactive kinase, was present (Fig. 7a). Moreover, HA-KEG levels appeared to decrease more rapidly over time in the presence as compared to the absence of CIPK26^{TD}-YFP-HA (Fig. 7a). These findings were replicated using a second *OlexA:CIPK26^{TD}-YFP-HA, 35S:HA-KEG/keg-1* transgenic insertion line (Fig. 7b). This observable difference in HA-KEG levels, over time, was quantified by analyzing the pixel intensity of immunoreactive bands on films used for detecting Western blots. The analysis revealed a more rapid decline in percent HA-KEG remaining over time in the induced versus the noninduced plants containing CIPK26^{TD}-YFP-HA (Fig. 7c). Taken together, the results suggest CIPK26 promotes the degradation of KEG.

3.2 CIPK26 is Implicated in the ABA-induced Degradation of KEG

A modified cycloheximide chase assay was carried out using *OlexA:CIPK26-YFP-HA, 35S:HA-KEG/keg-1* transgenic plants to determine if wild type CIPK26 overexpression affects the turnover of KEG in the presence of ABA. Seedlings were

treated with or without 17-β-estradiol to induce CIPK26-YFP-HA expression. Seedlings were then treated with CHX in the presence or absence of ABA. Plant tissue samples were collected at specified time points and an assessment of HA-KEG protein levels was made, by conducting immunoblot analysis with anti-HA antibodies. This allowed for a comparison of the effects of ABA and/or overexpression of CIPK26 on the rate of turnover of KEG. HA-KEG abundance was observed to be lower in ABA treated samples overexpressing CIPK26-YFP-HA, as compared to samples overexpressing CIPK26-YFP-HA without ABA treatment (Fig. 8a, b) and ABA treated samples not overexpressing CIPK26-YFP-HA (Fig. 8a). Overall, the degradation of HA-KEG protein was most substantial for ABA treated transgenic seedlings expressing CIPK26-YFP-HA. This finding indicates a role for CIPK26 in ABA-induced KEG degradation.

3.3 CIPK26, ABA Signaling, and Plant Response to ABA

CIPK26 overexpression renders *A. thaliana* plants hypersensitive to inhibition by ABA (Lyzenga et al., 2013). Consequently, it is believed that overexpression of a stabilized and constitutively active CIPK26 would result in further increased seedling sensitivity to ABA. To investigate this, primary root elongation of transgenic *35S:CIPK26-YFP-HA* and *35S:CIPK26^{TD}-YFP-HA* seedlings treated with or without ABA was studied. A comparison was made of percentage inhibition of primary root length in ABA-treated and untreated roots. Seedlings expressing CIPK26^{TD}-YFP-HA, a constitutively active form of CIPK26, appeared to be more highly sensitive to the inhibitory effects of ABA as compared to seedlings expressing the typical form of CIPK26, CIPK26-YFP-HA (Fig. 9a,b).

CIPK26 influences its own stability and phosphorylates KEG *in vitro* (Lyzenga et al., Unpublished results). These findings, coupled with the hypersensitivity of seedlings expressing CIPK26^{TD}-YFP-HA to ABA, support a model where, in the presence of ABA CIPK26 promotes KEG degradation, thereby enabling the accumulation of active CIPK26. To determine if ABA activates CIPK26, a phosphorylation assay was undertaken. For CIPKs to become fully activated, a site within the activation loop of the protein must be phosphorylated (Chaves-Sanjuan et al., 2014). *35S:CIPK26-YFP-HA* and *35S:CIPK26^{KR}-YFP-HA Arabidopsis thaliana* seedlings were used to study the phosphorylation state of CIPK26 in the presence versus absence of ABA (assays performed by Sam Campbell). A phospho-specific antibody used in Western blot analysis revealed higher-migrating forms of CIPK26 in the ABA treated and the untreated condition (Supplemental Fig. 1). This suggests CIPK26 is modified by phosphorylation in the presence and absence of ABA. Available mass spectrometry data indicates that CIPK26 possesses at least two residues that become phosphorylated (PhosPhAT Database) (Fig. 10a), and the CIPK26 sequence contains multiple predicted phosphorylation sites (NetPhos 2.0) (Fig. 10b). The effect of ABA may therefore be an altered phosphorylation pattern for the kinase.

3.4 NDL1 and XBAT32 Interact

A previous yeast-two hybrid screen indicated that XBAT32 and NDL1 interact with one another (Klopffleisch et al., 2011). Interaction mapping revealed that NDL1 interacts with several proteins, including XBAT32, which may be implicated in its regulation (Fig. 11). An *in vitro* glutathione S-transferase (GST) pull down assay

confirmed that NDL1 interacts with XBAT32 (Fig. 12). This finding was observed in multiple trials, however, non-specific binding of His-Flag-NDL1 to control glutathione agarose was apparent.

3.5 NDL1 is Degraded by the 26S Proteasome

Based on the finding of a probable interaction between NDL1 and a characterized E3 ligase, XBAT32, a subsequent line of questioning was whether the UPS is implicated in NDL1 turnover. To determine if the UPS targets NDL1, purified recombinant His-Flag-NDL1 was used with wild type Arabidopsis tissue in cell free degradation assays with MG132, an inhibitor of the 26S proteasome. Preliminary results indicated in the absence of MG132, His-Flag-NDL1 abundance decreased over time, however, in the presence of MG132, the rate of turnover of His-Flag-NDL1 decreased (Fig. 13).

3.6 NDL1 is Ubiquitinated

To investigate whether Arabidopsis NDL1 undergoes post-translational ubiquitin modification, ubiquitination site prediction software was first employed. Prediction software revealed that NDL1 contains multiple residues that could be ubiquitinated, and that ubiquitination of at least one of these sites is highly probable (Fig. 14a). To determine experimentally if NDL1 is ubiquitinated, pull-down assays were performed using p62-agarose beads, which bind and isolate ubiquitinated proteins using a ubiquitin-associated protein domain (UBP). If NDL1 is truly ubiquitinated, we anticipated that the p62-agarose would isolate the ubiquitin-modified form of the protein from total protein extract. Protein extract from *Arabidopsis thaliana* plants was mixed with purified recombinant His-Flag-

NDL1 and together they were incubated with p62-agarose. Western blot analyses with anti-Flag antibodies revealed a ubiquitinated form of NDL1 among p62-agarose protein isolates (Fig. 14b, Supplemental Fig. 2), at molecular weights corresponding to the predicted molecular weight of modified NDL1. This finding is indicative of the modification of NDL1 by ubiquitination and provides further reason to believe NDL1 is regulated by the UPS.

3.7 XBAT32 is Implicated in NDL1 Degradation

The findings that NDL1 and XBAT32 interact, and that NDL1 turnover is 26S proteasome dependent suggest a role for XBAT32 in targeting NDL1 for degradation. In order to investigate XBAT32 involvement in NDL1 degradation by the 26S proteasome, protein extracts from wild type or *xbat32-1* seedlings and His-Flag-NDL1 were employed in cell free degradation assays. The rate of degradation of His-Flag-NDL1 was compared between the two assays. Preliminary immunoblot analyses with anti-Flag antibodies indicated that His-Flag-NDL1 was turned over more rapidly in extracts from wild type seedlings as compared to *xbat32-1* seedlings (Fig. 15). Little change was observed in His-Flag-NDL1 stability when MG132 was added to extracts from *xbat32-1* plants (Fig. 15). The data suggest a role for the E3 ligase XBAT32 in mediating NDL1 degradation via the 26S proteasome.

Figure 6. CIPK26 promotes KEG degradation in a cycloheximide chase assay. *In planta* CHX chase assay using 5-day-old *OLexA:CIPK26^{TD}-YFP-HA,* 35S:HA-KEG/keg-1 (line 1) and *OLexA:CIPK26^{KR}-YFP-HA, 35S:HA-KEG/keg-1* (line 1) *Arabidopsis thaliana* plants. Seedlings were incubated in liquid growth medium supplemented with (+) or without (-) 20 μM 17-β-estradiol to induce expression of CIPK26, treated with CHX and samples were collected at the indicated time points. The abundance of HA-KEG present at each time point was determined by Western blotting (WB) with HA antibodies. Protein determination was made by the Bradford assay. Ponceau S staining was used to confirm even protein loading. a) Trial 1, compare lanes 5 and 6 to lanes 2 and 3, and compare lanes 5 and 6 to lanes 8 and 9. b) Trial 2, compare lane 4 to lane 2, and compare lane 4 to lane 6.

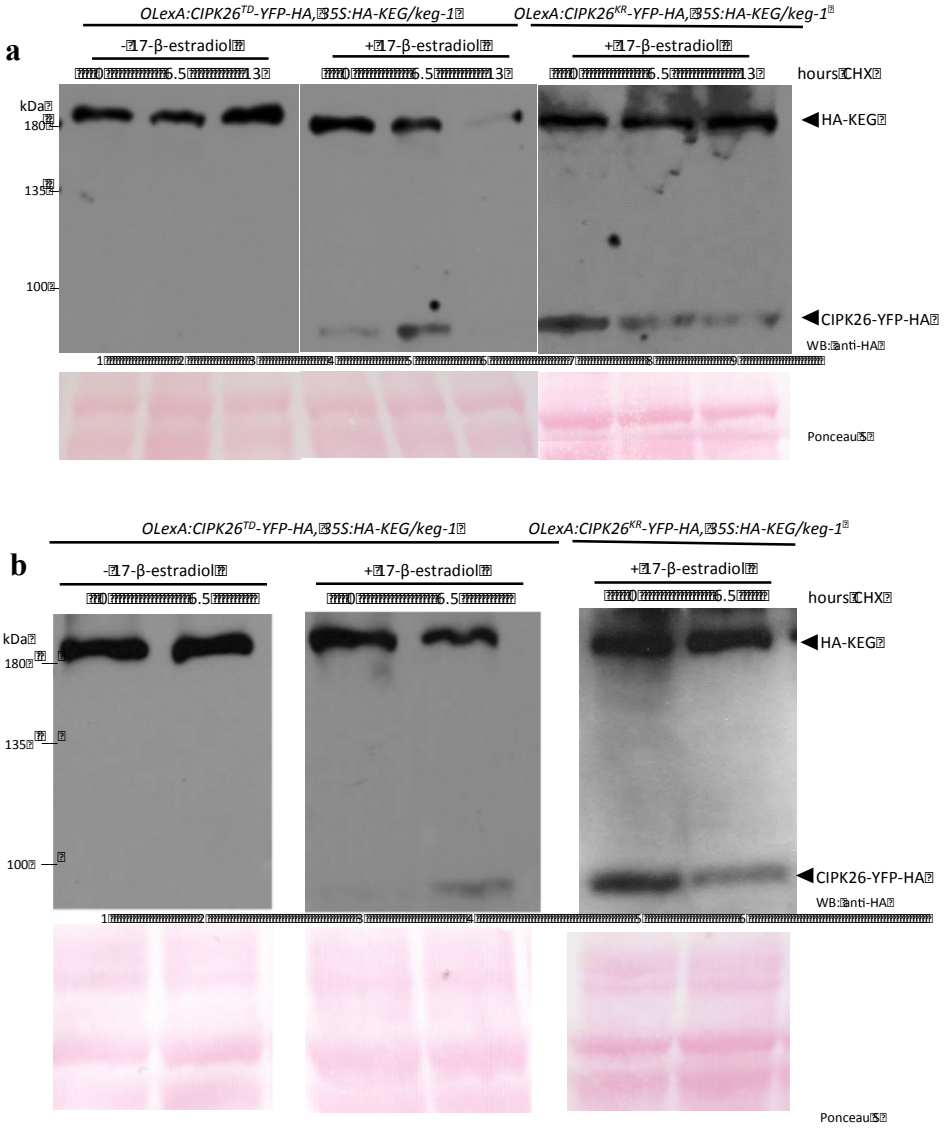
a
OLexA:CIPK26TD-YFP-HA,35S:HA-KEG/keg-1
OLexA:CIPK26KR-YFP-HA,35S:HA-KEG/keg-1
-17-β-estradiol
+17-β-estradiol
+17-β-estradiol
hours CHX
kDa
180
135
100
HA-KEG
CIPK26-YFP-HA
WB: anti-HA
Ponceau S
b
OLexA:CIPK26TD-YFP-HA,35S:HA-KEG/keg-1
OLexA:CIPK26KR-YFP-HA,35S:HA-KEG/keg-1
-17-β-estradiol
+17-β-estradiol
+17-β-estradiol
hours CHX
kDa
180
135
100
HA-KEG
CIPK26-YFP-HA
WB: anti-HA
Ponceau S

Figure 7. CIPK26 affects KEG stability in cell free degradation assays. Constitutively active CIPK26 promotes the degradation of KEG in a cell free assay. a) Cell free degradation assay using protein extracts from 5-day-old *OLexA:CIPK26^{TD}-YFP-HA, 35S:HA-KEG/keg-1* (line 1) and *OLexA:CIPK26^{KR}-YFP-HA, 35S:HA-KEG/keg-1* (line 1) seedlings previously induced to express CIPK26 with 20 μM 17-β-estradiol. HA-KEG protein abundance was determined by Western blotting (WB) using HA antibodies on samples from the indicated time points. Ponceau S staining was used to confirm equal protein loading. b) Cell free degradation assay using protein extracts from 5-day-old *OLexA:CIPK26^{TD}-YFP-HA, 35S:HA-KEG/keg-1* (line 2) seedlings and *OLexA:CIPK26^{KR}-YFP-HA, 35S:HA-KEG/keg-1* (line 1) seedling induced to express CIPK26 with 20 μM 17-β-estradiol. HA-KEG protein abundance was determined by Western blotting (WB) using HA antibodies on samples from the indicated time points. Ponceau S staining was used to confirm even sample loading. c) Line graph represents percent HA-KEG remaining over time. Percent remaining is the percent of HA-KEG remaining at each time point taken from a and b and averaged for the two plant lines, ± standard error of the mean. Red line represents samples from seedlings not treated with 17-β-estradiol, not expressing CIPK26^{TD}-YFP-HA, pink line represents samples from seedlings treated with 17-β-estradiol, expressing CIPK26^{TD}-YFP-HA. Quantification of band intensity was conducted using ImageJ software where image was converted to 16-bit grey scale and pixel intensity values were measured using the analyze particles function (Abramoff et al., 2004). Percent remaining was determined by comparing pixel intensity values at each time point to those at the zero time point.

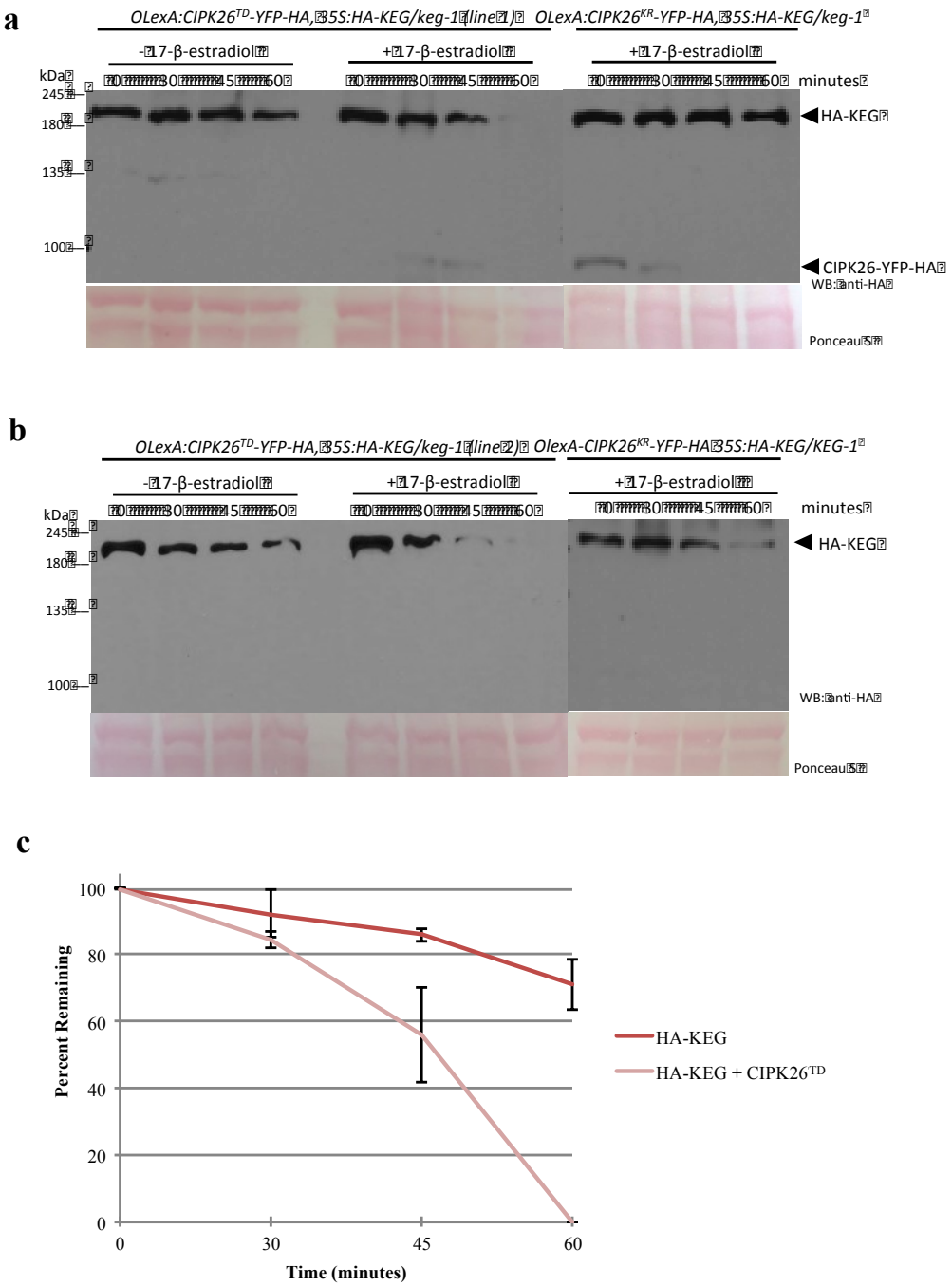
a
OLexA:CIPK26TD-YFP-HA,35S:HA-KEG/keg-1 (line 1)
OLexA:CIPK26KR-YFP-HA,35S:HA-KEG/keg-1
-17-β-estradiol
+17-β-estradiol
+17-β-estradiol
kDa
245
180
135
100
0 30 45 60
0 30 45 60
0 30 45 60
minutes
HA-KEG
CIPK26-YFP-HA
WB: anti-HA
Ponceau S
b
OLexA:CIPK26TD-YFP-HA,35S:HA-KEG/keg-1 (line 2)
OlexA-CIPK26KR-YFP-HA35S:HA-KEG/KEG-1
-17-β-estradiol
+17-β-estradiol
+17-β-estradiol
kDa
245
180
135
100
0 30 45 60
0 30 45 60
0 30 45 60
minutes
HA-KEG
WB: anti-HA
Ponceau S
c
Percent Remaining
100
80
60
40
20
0
0
30
45
60
Time (minutes)
HA-KEG
HA-KEG + CIPK26TD

Figure 8. CIPK26 is implicated in the ABA-induced degradation of KEG. KEG degradation occurs at an elevated rate in the presence of CIPK26 and ABA. 5-day-old *OLexA:CIPK26-YFP-HA, 35S:HA-KEG/keg-1* seedlings were incubated in liquid growth medium either without (-) or with (+) 20 μM 17-β-estradiol added. Seedlings were then treated without (-) or with (+) ABA and cyclohexamide (CHX) and samples were collected at the indicated time points. HA-KEG levels at each time point were determined by the immunoprobing of Western blots (WB) with HA antibodies. Ponceau S staining was used to confirm equal loading. a) Trial 1 b) Trial 2

a

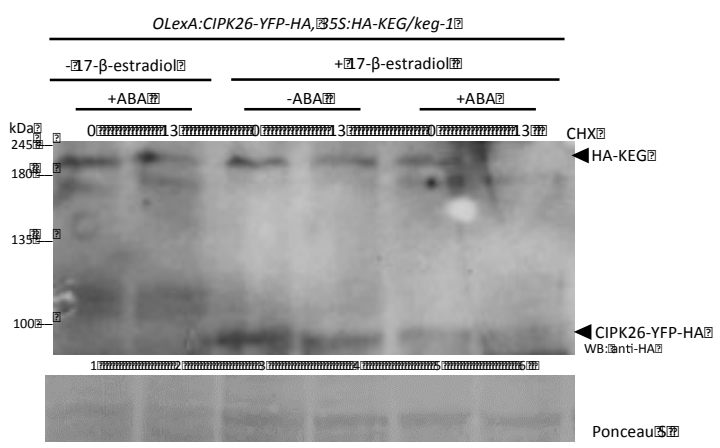
OLexA:CIPK26-YFP-HA, 35S:HA-KEG/keg-1
-17-β-estradiol
+17-β-estradiol
+ABA
-ABA
+ABA
kDa
245
180
135
100
CHX
HA-KEG
CIPK26-YFP-HA
WB: anti-HA
Ponceau S

b

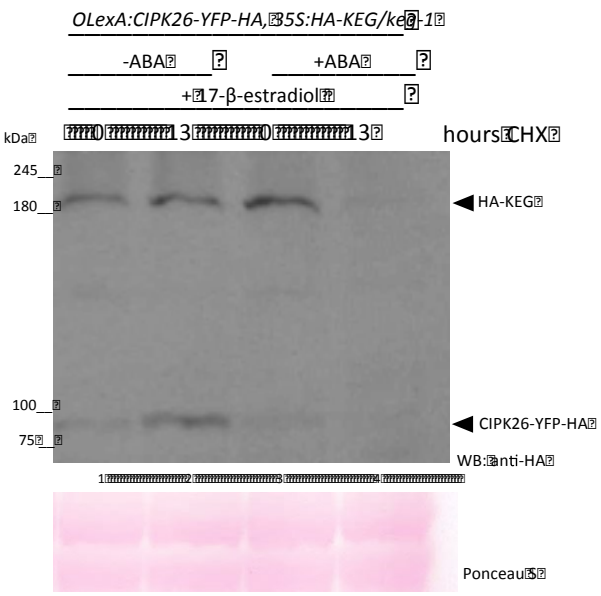
OLexA:CIPK26-YFP-HA, 35S:HA-KEG/keg-1
-ABA
+ABA
+17-β-estradiol
kDa
hours CHX
245
180
100
75
HA-KEG
CIPK26-YFP-HA
WB: anti-HA
Ponceau S

Figure 9. Seedlings possessing constitutively active CIPK26 are hypersensitive to ABA. a) Representative 9-day-old *35S:CIPK26-YFP-HA* (line 1) and *35S:CIPK26^{TD}-YFP-HA* (line 1) transgenic seedlings were grown 4 days without ABA and then grown on media supplemented with 5μM ABA for 5 days. b) Graph illustrating the percentage inhibition in primary root length between ABA-treated and untreated transgenic *35S:CIPK26-YFP-HA* (line 1) and *35S:CIPK26^{TD}-YFP-HA* (line 1) seedlings. Primary root length was monitored every 24 h and assessed by ImageJ analysis after 3 and 5 days post-transfer. Bars represent percentage inhibition calculated from two separate trials, with a minimum of 6 seedlings per trial, n = 12. *35S:CIPK26-YFP-HA* appears to be notably different from *35S:CIPK26^{TD}-YFP-HA* 5 days post transfer. Error bars represent mean ± SE.

a

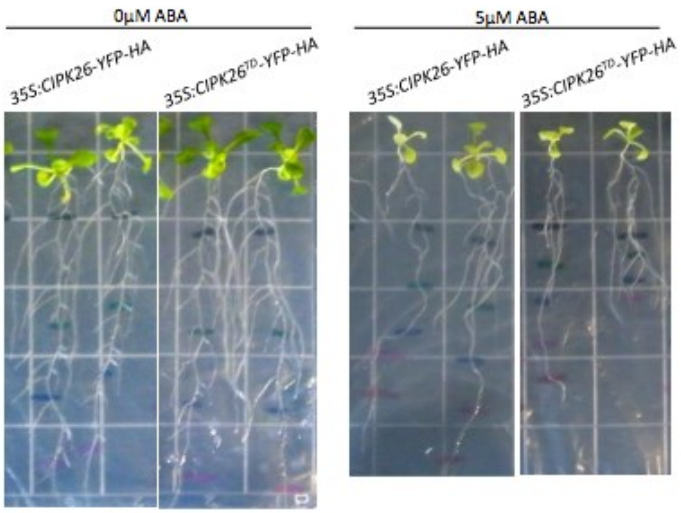
0μM ABA
5μM ABA
35S:CIPK26-YFP-HA
35S:CIPK26TD-YFP-HA
35S:CIPK26-YFP-HA
35S:CIPK26TD-YFP-HA

b

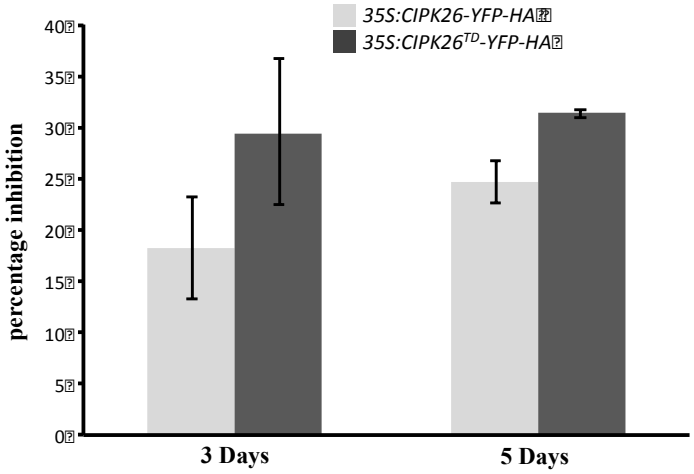
35S:CIPK26-YFP-HA
35S:CIPK26TD-YFP-HA
percentage inhibition
40
35
30
25
20
15
10
5
0
3 Days
5 Days

Figure 10. CIPK26 is phosphorylated at multiple sites. a) The sequence of CIPK26 has two experimentally determined phosphorylated residues, determined by mass spectrometry analysis, according to the PhosPhAT 4.0 database. CIPK26 sequence is displayed and the known phosphorylated residues are highlighted in brown. b) NetPhos 2.0 software predicted that CIPK26 contains as many as 13 potentially phosphorylated residues; 6 serine phosphorylation sites, 4 threonine phosphorylation sites, and 3 phosphorylated tyrosine sites. CIPK26 sequence is displayed and predicted phosphorylated residues are highlighted in green.

a

b

Figure 11. N-MYC DOWNREGULATED-LIKE 1 (NDL1) and XBAT32 are potential interactors. A previous high-throughput yeast-two hybrid screen identified NDL1 and XBAT32 as potential interaction partners. BioGRID interaction data is aggregated through publication searches. BioGRID interaction maps represented here display potential interactors of NDL1 and XBAT32. a) NDL1 interactors; XBAT32 is a proposed interactor of NDL1, circled in orange. b) XBAT32 interactors; NDL1 is a proposed interactor of XBAT32, circled in red.

a

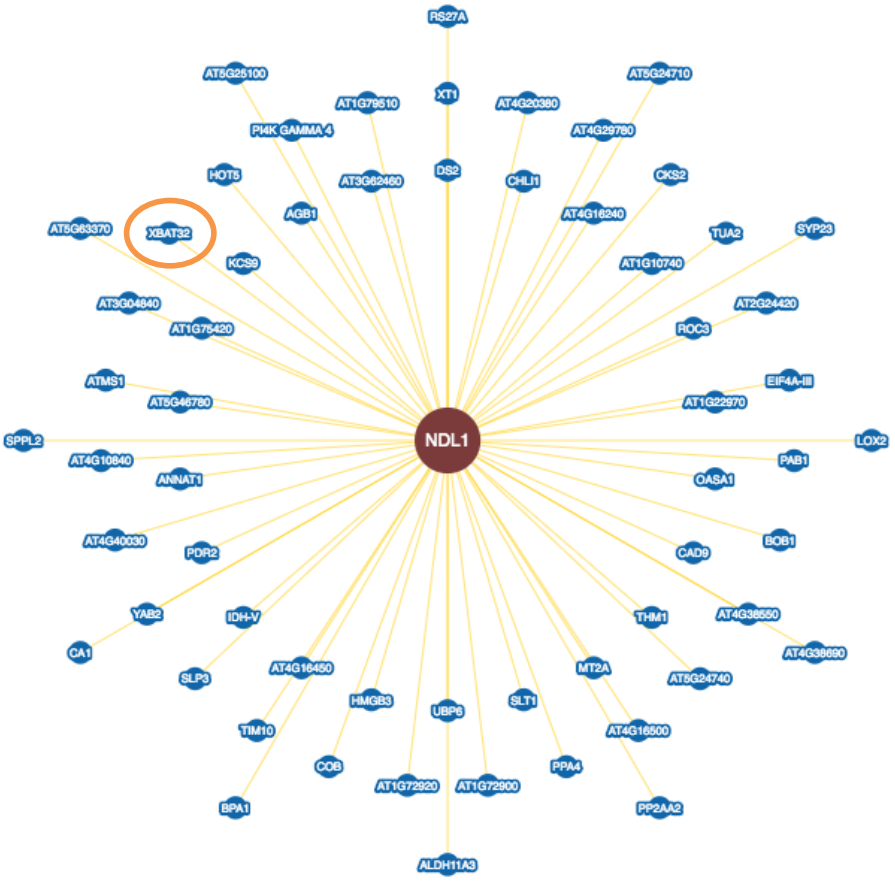
RS27A
AT5G25100
AT1G79510
XT1
AT4G20380
AT5G24710
PI4K GAMMA 4
AT4G29780
HOT5
AT3G62460
DS2
CHLI1
CKS2
AT5G63370
XBAT32
AGB1
AT4G16240
TUA2
SYP23
KCS9
AT1G10740
AT3G04840
AT2G24420
AT1G75420
ROC3
ATMS1
EIF4A-III
AT5G46780
AT1G22970
SPPL2
NDL1
LOX2
AT4G10840
PAB1
ANNAT1
OASA1
AT4G40030
PDR2
CAD9
BOB1
YAB2
IDH-V
THM1
AT4G38650
CA1
AT4G38690
SLP3
AT4G16450
MT2A
AT5G24740
HMGB3
UBP6
SLT1
TIM10
AT4G16500
COB
PPA4
AT1G72920
AT1G72900
BPA1
PP2AA2
ALDH11A3

b

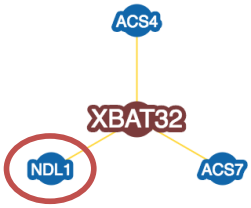
ACS4
XBAT32
NDL1
ACS7

Figure 12. NDL1 and XBAT32 interact in a GST Pull down Assay. His-GST-XBAT32 and His-GST were immobilized separately on glutathione-agarose. Beads were incubated with total bacterial cell (Rosetta) lysate expressing recombinant His-Flag-NDL1. Blots reveal the result of incubation of His-Flag-NDL1 with His-GST-XBAT32 beads or His-GST beads. Top panel indicates that more His-Flag-NDL1 was isolated following incubation with glutathione-agarose with His-GST-XBAT32 immobilized compared to with His-GST alone immobilized. His-Flag-NDL1 is represented by grey arrowhead. Anti-Flag antibodies were used in Western blotting. Bottom panel indicates that His-GST-XBAT32 and His-GST were immobilized on glutathione-agarose, respectively. Lane labeled as His-GST-XBAT32 represents approximately $1/10^{th}$ of the fraction of His-GST-XBAT32 beads incubated with His-Flag-NDL1 lysate, lane labeled His-GST is representative of approximately $1/20^{th}$ of the fraction of His-GST beads incubated with His-Flag-NDL1. The His-GST tagged XBAT32 is indicated by * and His-GST by the black arrowhead. Anti-GST antibodies were used for immunoblotting.

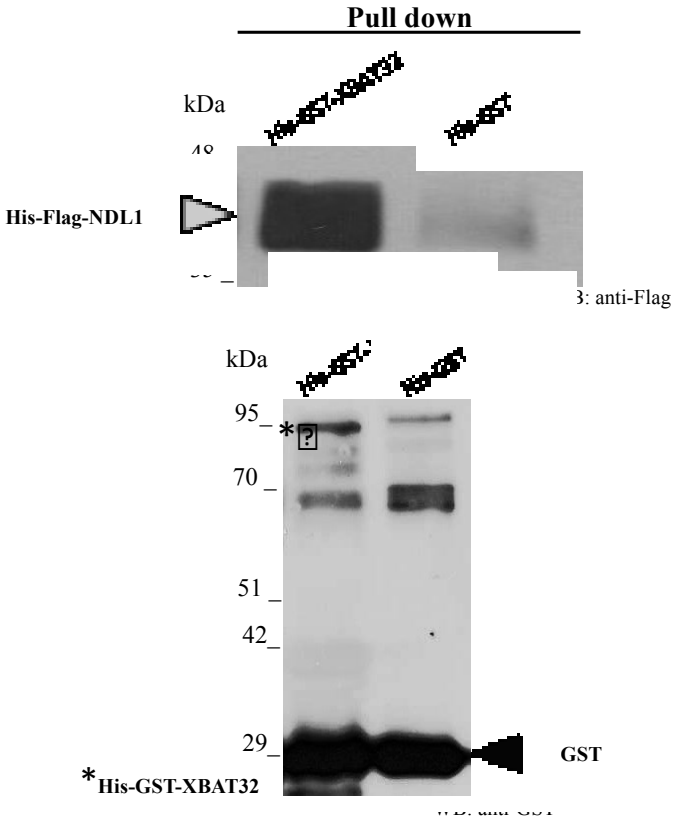
Pull down
kDa
His-Flag-NDL1
kDa
95_
70 _
51 _
42_
29_
*His-GST-XBAT32
GST

Figure 13. NDL1 is degraded by the 26S proteasome. Cell free degradation assays were performed with wild type *Arabidopsis thaliana* protein extracts and purified recombinant His-Flag-NDL1. His-Flag-NDL1 was mixed with protein extract from wild type *A. thaliana* with (+) or without (-) 50 μM of MG132. Panel on left hand side indicates samples without (-) MG132, panel on right hand side indicates samples with (+) MG132. Times at which samples were taken from the total cell free reaction are indicated in minutes. Black arrowhead indicates His-Flag-NDL1 protein. Anti-Flag antibodies were used for immunoprobing of Western blots, allowing for detection of relative abundance of His-Flag-NDL1 remaining at each time point. Ponceau S staining was used to verify equal protein loading.

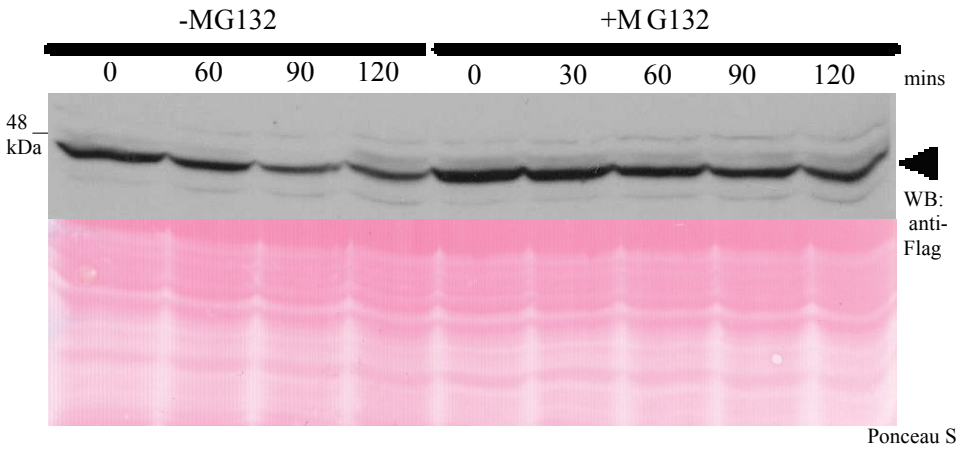
-MG132
+MG132
0
60
90
120
0
30
60
90
120
mins
48
kDa
WB:
anti-
Flag
Ponceau S

Figure 14. NDL1 is ubiquitinated in a semi-*in vitro* assay. a) UbiProber, iUbiq-Lys, and BDM-PUB were employed to predict ubiquitination sites on NDL1. Software returned a prediction of 6 ubiquitinated sites (1 with high probability), 1 ubiquitinated site, and 8 ubiquitinated sites (2 with high probability), respectively. NDL1 sequence is displayed and predicted ubiquitinated sites are highlighted in yellow. Brown box indicates the site with the highest likelihood of being ubiquitinated. b) Purified recombinant His-Flag-NDL1 was used in semi-*in vitro* ubiquitination assays in combination with total protein extract from wild type *Arabidopsis thaliana* seedlings. Numbers beneath blots indicate Lanes. His-Flag-NDL1 was detected by immunoprobing with anti-Flag antibodies and is represented in lane 1. In lane 3, this purified His-Flag-NDL1 was added to total Arabidopsis protein extracts and incubated with p62-agarose (ubiquitin-trap beads) for 4 h at 4 °C. In lane 2, purified His-Flag-NDL1 was not added to Arabidopsis protein extracts incubated with p62-agarose for 4 h at 4 °C. Western blot analysis with anti-Flag antibodies revealed that p62-agarose isolated ubiquitin-modified His-Flag-NDL1 in lane 3. * indicates non-specific binding. Col-0 is Columbia ecotype.

a

```
  1 MTDSYGAVSV DVGTIYLGGK EHRVKTASGV VSVIVYGDRE KPALITYPDL
 51 ALNHMSCFQG LFFCPEAASL LLHNFCIYHI SPPGHELGAA PICPNDSVPS
101 AENLADQILE VLNFFGLGVV MCMGVTAGAY ILTLFAMKHR ERVLGLILVS
151 PLCKAPSWSE WFYNKVITNLLYYYGMCGVV KEFLLQRYFS KEVRGNVEIP
201 ESDIAQACRR LLDERQGINV LRFLDAIDRR PDISSGLKKL KCRTLIFIGD
251 QSPFYSEAVH MAATLDRGYC ALVEVQACGS MVTEEQPHAM LIPMEYFLMG
301 YGLYRPSLFS ESPRSPLSPS CISPELLSPE SMGLKLKPIK TRISAA
```

b

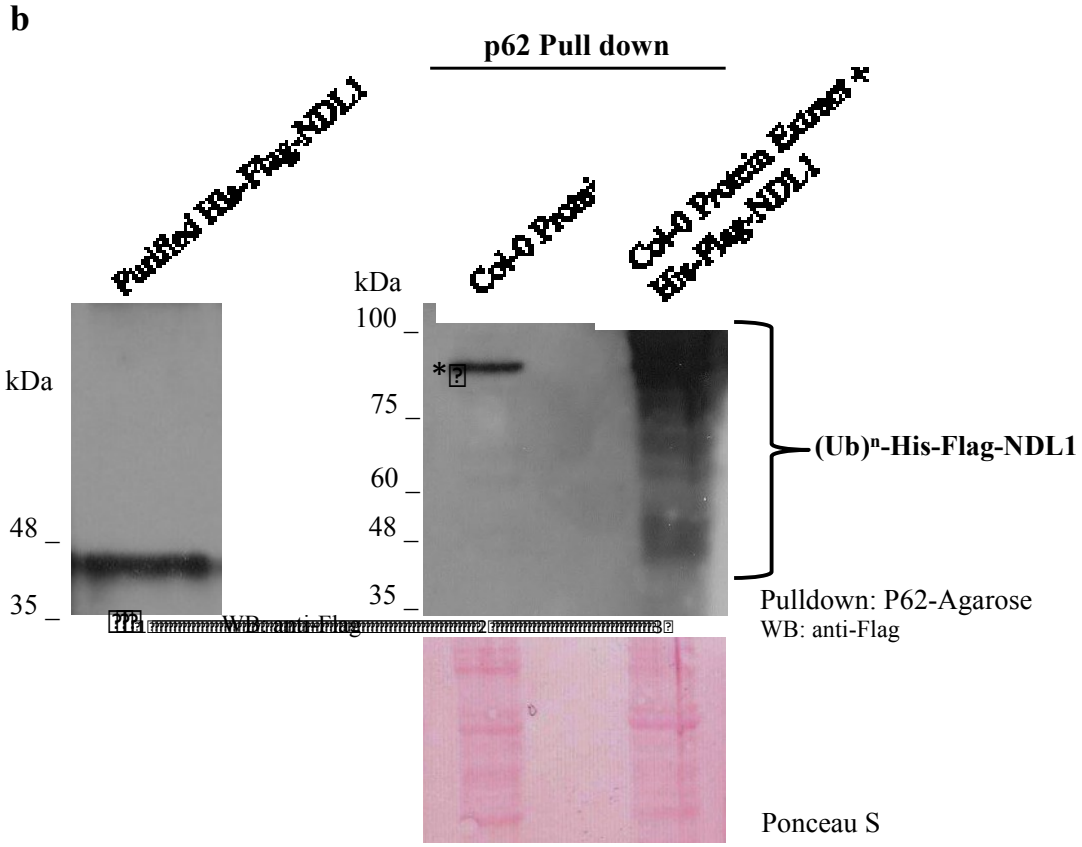

Figure 15. Cell free degradation assays suggest XBAT32 is implicated in NDL1 degradation. Preliminary cell free degradation assays were performed with *Arabidopsis thaliana* protein extracts from wild type (wt) and *xbat32-1* plants, and purified His-Flag-NDL1. His-Flag-NDL1 was mixed with total protein extract with (+) or without (-) 50 μM of MG132. Time at which samples were removed from cell free reactions is indicated in minutes. His-Flag-NDL1 remaining at each time point was detected by immunoprobing of Western blots (WB) with anti-Flag antibodies. Black arrowhead indicates His-Flag-NDL1. His-Flag-NDL1 appears more stable in the *xbat32-1* background, as compared to the wt background in the absence of a proteasome inhibitor. Ponceau S staining shows equal protein loading.

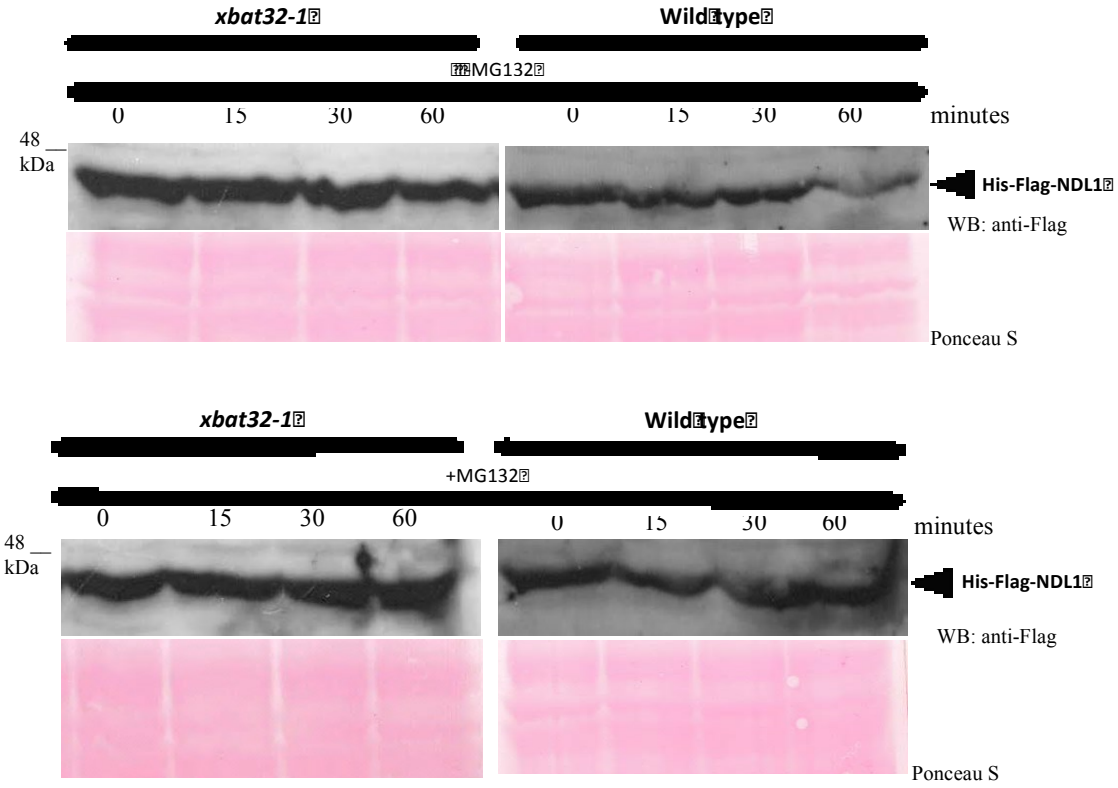
xbat32-1
Wild type
MG132
0
15
30
60
0
15
30
60
minutes
48
kDa
His-Flag-NDL1
WB: anti-Flag
Ponceau S
xbat32-1
Wild type
+MG132
0
15
30
60
0
15
30
60
minutes
48
kDa
His-Flag-NDL1
WB: anti-Flag
Ponceau S

CHAPTER 4: DISCUSSION

Intricate networks of proteins, including transcription factors and enzymes tightly regulate hormone signaling and responses in plants. With this work I provide further evidence for a counter-regulatory relationship between the E3 ligase KEG and the kinase CIPK26 during abscisic acid signaling. Moreover, I present data to indicate a relationship between the E3 XBAT32, involved in ethylene signaling, and NDL1, a G-protein effector implicated in the formation of auxin gradients.

4.1 Regulation of NDL1 Stability by XBAT32 through Ubiquitination

A high throughput yeast-two hybrid (Y2H) screen previously identified N-MYC DOWNREGULATED-LIKE-1 (NDL1) as a potential interactor of the characterized RING-type E3 ligase XBAT32 (Klopffleisch et al., 2011). In this work I studied the potential interaction between XBAT32 and NDL1, and investigated if the UPS has a role in NDL1 regulation. In order to supplement this Y2H evidence suggesting an interaction, a GST-pull down assay was performed, which demonstrated that NDL1 binds XBAT32 (Fig. 12). While the GST-pull down assay was an *in vitro* assay, it is reasonable to suggest that this interaction occurs in an *in planta* system. Both XBAT32 and NDL1 display high expression in flower and root tissues, in particular (Mudgil et al., 2009). Previous reports suggest NDL1 localizes to the cytoplasm, specifically to punctate cytoplasmic structures (Mudgil et al., 2009), and XBAT32 is thought to localize to cellular membranes (Nodzon et al., 2004). While the E3 and its potential target appear to be differentially localized, this does not preclude interaction between the two, and there are many examples of E3 ligases that regulate substrates localized to subcellular compartments different than the one they occupy. One example is the regulation of ABI5,

which resides in the nucleus, by KEG, a trans-Golgi network and cytosolic protein (Gu & Innes, 2011; Lopez-Molina et al., 2002). KEG and ABI5 interact directly in the cytoplasm and the trans-Golgi network (Liu & Stone, 2013). In addition, an interaction between a cytoplasmic protein, like NDL1, and one situated at cellular membranes, like XBAT32, could be explained by protein shuttling, further suggesting a physical interaction between the two proteins is feasible.

NDL1 is similar to its animal equivalent, N-MYC DOWNREGULATED GENE 1 (NDRG1) and it is thought to serve related roles in animals and plants (Khatri & Mudgil, 2015). Likewise, NDRG1 and NDL1 share multiple interactors implicated in common pathways (Khatri & Mudgil, 2015). NDRG1 is post-translationally modified by Small Ubiquitin-like Modifier (SUMO), specifically by SUMO-2, affecting the stability of NDRG1 (Lee & Kim, 2015). This modulation of NDRG1 abundance and functionality by a Small Ubiquitin-like Modifier suggests the possibility that NDL1 stability and function are also regulated by a similar post-translational modification. Previous work by Mudgil et al., 2009, using β-glucuronidase (GUS) staining, also suggests that NDL1 is regulated post-translationally. Here, using ubiquitylation site prediction software (UniProber, iUbiq-Lys, and BDM-PUB), I investigated the possibility that NDL1 has residues that can become ubiquitinated. Prediction software indicated that at least one NDL1 residue has a high likelihood of being ubiquitinated (Fig. 14a). Additionally, using p62-agarose beads that preferentially bind ubiquitinated proteins, higher migrating forms of His-Flag-NDL1 were isolated in a semi-*in vitro* ubiquitin pull down assay (Fig. 14b, Supplemental Fig. 2). This serves as strong evidence that NDL1 is ubiquitinated.

In the literature, there also exists evidence to suggest a protease is implicated in controlling NDL1 protein levels (Mudgil et al., 2009). Here, using cell free degradation

assays, we provide further evidence that NDL1 is likely degraded by the 26S proteasome (Fig. 13). However, this finding will need to be replicated. The Gβ subunit (AGB1) of the heterotrimeric G protein complex is involved in regulating the post-translational stability of NDL1, being necessary for the accumulation of high levels of NDL1 in primary and lateral root meristems (Mudgil et al., 2009). This was determined by assessing NDL1 abundance and stability in Arabidopsis plants lacking AGB1 (Mudgil et al., 2009). My results suggest that XBAT32 is also involved in regulating NDL1 stability (Fig. 15) via XBAT32 E3 ligase activity and the UPS.

4.1.1 Support for a Model Connecting XBAT32, NDL1, Ethylene, and Auxin

Arabidopsis NDL proteins positively regulate primary root development, meristem initiation and branching, and lateral root formation, by modulating auxin transport and gradients, and the abundance of two specific auxin transport facilitators (Mudgil et al., 2009; Mudgil et al., 2013). NDL1 ultimately modulates auxin gradients essential for normal development, including lateral root development (Mudgil et al., 2013). On the other hand, XBAT32 is implicated in the control of ethylene biosynthesis, by negatively regulating the abundance of enzymes involved in the rate-limiting step of ethylene biosynthesis (Prasad et al., 2010). Ethylene suppresses lateral root development by preventing localized auxin accumulation, which promotes initiation of root branching and lateral root development (Negi et al., 2008). Therefore, NDL1 and XBAT32 converge on auxin transport, and both are implicated in the production of lateral roots.

Appropriate auxin biosynthesis, signaling and transport are crucial for normal lateral root development (Péret et al., 2009). Reduction in NDL gene expression, or overexpression of NDL1 affects root architecture, auxin transport and auxin maxima

(Mudgil et al., 2009). The overexpression of NDL1 increases the abundance of lateral roots, while the absence of NDL yields fewer lateral roots (Mudgil, 2009). This altered lateral root phenotype may be explained by mutations in *NDL* resulting in altered auxin transport and aberrant root auxin gradients (Mudgil et al., 2009). This aspect of the mutant *ndl* phenotype mimics a feature of the phenotype observed for *xbat32-1* plants, which is the production of significantly fewer lateral roots than the wild type (Nodzon et al., 2004; Prasad et al., 2010). In the case of *xbat32-1* seedlings, an increase in ethylene production inhibits lateral root development, possibly by altering auxin transport and preventing its accumulation (Negi et al., 2008; Lewis et al., 2011; Prasad et al., 2010).

Based on my finding that NDL1 is likely to be regulated in part by XBAT32, the similarity between *xbat32* and *ndl* mutant phenotypes is unexpected, and it would be anticipated that NDL1 and XBAT32 mutants have opposite phenotypes. This is an observation that remains to be reconciled but one possible explanation may be the effect of the relationship between NDL1, AGB1, sugar, and auxin on XBAT32's regulation of NDL1. AGB1 and NDL1 function together in signaling pathways and NDL1, AGB1, and auxin may cooperate through feedback loops in order to tightly regulate auxin gradients and transport (Mudgil et al., 2009). Moreover, there is potential crosstalk between sugar and AGB1 in the regulation of NDL1 root levels (Mudgil et al., 2009). The intricate network of elements, and potentially unknown elements, involved in the regulation of NDL1 may help to explain why *xbat32* and *ndl* do not have opposing phenotypes. A second, related, possibility is that the abundance and localization of auxin is critical for NDL1 regulation, and varying concentrations or localizations of auxin could have similar detrimental effects on lateral root development. A third explanation may be related to the feedback regulation of XBAT32, for which there is conflicting evidence. Previous

analyses on a potential ethylene and/or auxin feedback loop acting on XBAT32 returned conflicting results. One analysis found that ethylene repressed XBAT32 expression in an auxin-dependent manner, while another study determined that auxin increased XBAT32 expression (Prasad et al., 2010; Nodzon et al., 2004) (Fig. 16). The relationship of XBAT32 and NDL1 with auxin and ethylene is thus complex, and in light of conflicting evidence for feedback regulation of XBAT32, and similar mutant phenotypes observed for *xbat32-1* and *ndl* plants, it is an area for future exploration.

The work presented here suggests that XBAT32 not only plays a role in lateral root formation through an effect on ethylene biosynthesis, but that it regulates lateral root development by regulating NDL1 abundance and stability (Fig. 16). Where lateral root development is concerned, XBAT32 is likely to sit at a crossroads regulating ethylene production, while simultaneously regulating NDL1, and therefore regulating the response to ethylene. By establishing a link between XBAT32 and NDL1, the work herein further supports a role for XBAT32 in regulating crosstalk between auxin and ethylene in order to control lateral root development.

4.1.2 Self-Regulation and Auto-Ubiquitination of RING-Type E3 Ligases

XBAT32 is a characterized E3 ubiquitin ligase with the capacity to self-regulate through self-ubiquitination. It was previously demonstrated that XBAT32 is capable of regulating its own stability through autoubiquitination, which leads to subsequent proteasomal degradation of the E3 (Nodzon et al., 2004). A common trait of RING-type E3 ligases is their capacity to catalyze their own ubqiuitination (Huibregste et al., 1995; De Bie & Ciechanover, 2011; Lorick et al., 1999). This ability of RING-type E3s to self-ubiquitinate has also been demonstrated for other XBAT family members, including

XBAT35.2, which is thought to autoubiquitinate in an effort to maintain basal levels of the E3 until such time as a stimulus is present, for example a pathogen (McVey, 2015). While the functions of E3 self-ubiquitination are just beginning to be characterized, we can suggest XBAT32 autoubiquitination may function in periods of development when ethylene levels rise. An area for future research is the exploration of uses for RING-type E3 ligase autoubiquitination.

Figure 16. Representation of the relationship between XBAT32 and NDL1. Solid lines are indicative of demonstrated relationships, dotted lines represent proposed relationships or those for which conflicting evidence exists. XBAT32 regulates ethylene biosynthesis by controlling the stability of ACSs. Ethylene suppresses lateral root development through a mechanism implicating auxin. Auxin promotes lateral root development. NDL1 modulates auxin gradients. NDL1 and XBAT32 are mutually involved in auxin regulation, as well as lateral root formation. XBAT32 is likely implicated in the regulation of NDL1 stability and NDL1 turnover is ubiquitin-proteasome system dependent. Auxin treatment induces expression of the XBAT32 gene and is thought to have a negative effect on NDL1 stability in the region of the root apical meristem.

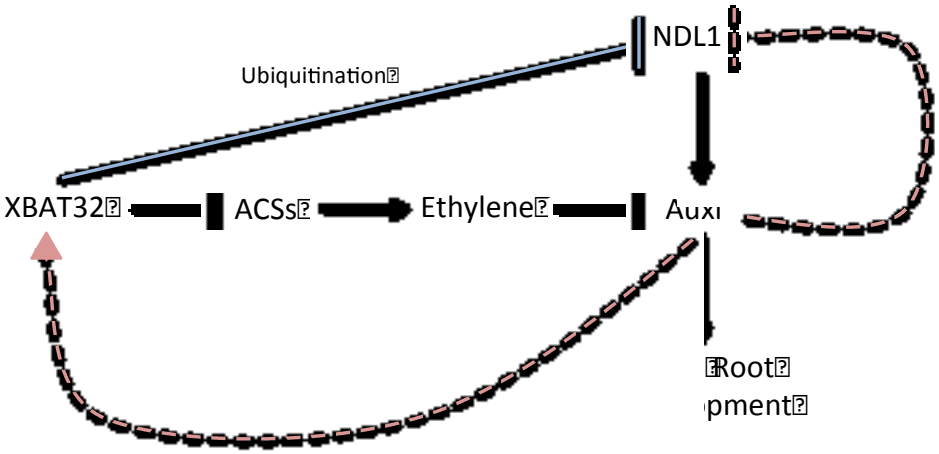
NDL1
Ubiquitination
XBAT32
ACSs
Ethylene
Root
pment

4.2 The Effect of CIPK26 Kinase Activity on Itself and on KEG E3 Ligase

A link between KEG, an E3 ligase, and CIPK26, a kinase involved in ABA signaling, was previously established (Lyzenga et al., 2013). It was demonstrated that KEG is involved in targeting the kinase CIPK26 for ubiquitination and degradation via the 26S proteasome, in the absence of the hormone ABA (Lyzenga et al., 2013). Additionally, it was previously known that in the presence of ABA, a phosphorylation event on KEG leads KEG to self-regulate through autoubiquitination, resulting in KEG degradation (Liu & Stone, 2010). However, conditions affecting CIPK26 stability had not previously been investigated, nor had the upstream signaling events leading to KEG phosphorylation and self-ubiquitination. More recently, unpublished work by Wendy Lyzenga (2016) suggested a role for the kinase activity of CIPK26 in regulating its own stability, and the stability of KEG. Specifically, Lyzenga (2016) demonstrated that active CIPK26, mutated to be constitutively active, displays increased stability, as compared to the unmodified kinase or the kinase inactive form of the protein, that ABA alters KEG's phosphorylation profile, and that CIPK26 has the capacity to phosphorylate KEG *in vitro* (Lyzenga et al., 2016). This study was conducted in order to fill a gap in the knowledge relating to the characterization of the interaction between KEG and CIPK26. Here, I provide *in planta* and cell free evidence to show that CIPK26 kinase activity regulates KEG stability and promotes KEG degradation, utilizing cell free degradation assays and cycloheximide chase assays. This serves as convincing evidence to suggest a counter-regulatory relationship between KEG and CIPK26, where KEG and CIPK26 regulate the activity of one another. Due to the fact that CIPK26 was found to affect KEG stability, it was reasonable to hypothesize CIPK26 would serve a role in ABA dependent KEG degradation. I demonstrate here that CIPK26 is also implicated in the ABA-induced

degradation of KEG.

Regulation of CIPK activity and stability is complex. In addition to being regulated by ubiquitination, CIPK activity is also controlled by self-inhibitory NAF domains, as well as by phosphorylation (Yu et al., 2014). In order for these kinases to become fully activated, they must interact with phosphorylated CBL proteins, and be phosphorylated on their activation loop (Hashimoto et al., 2012; Chaves-Sanjuan et al., 2014). Phosphorylation can prevent ubiquitination and affect E3 ligase activity (Hunter, 2007). When ubiquitination targets become phosphorylated it affects particular modular binding domains, which results in the generation or destruction of phosphodegrons. I aimed to investigate the phosphorylation and activation state of CIPK26, in the presence and absence of ABA. It was anticipated that treatment with ABA would result in an activated and phosphorylated form of CIPK26. However, analysis using phospho-specific antibodies revealed a phosphorylated form of CIPK26 in both the presence and absence of ABA (Supplemental Fig. 1). Helping to explain this unexpected result was the finding that CIPK26 has two experimentally determined (by mass spectrometry) phosphorylation sites, in addition to multiple predicted phosphorylation sites (Fig. 10). Together, these results indicate that CIPK26 is phosphorylated in both the presence and the absence of ABA, but that there may be a difference in which CIPK26 sites are phosphorylated in one condition versus the other. Another possible explanation for this finding is that, as a result of using seedlings overexpressing CIPK26, some CIPK26 may be capable of escaping typical regulation by clade A type 2C phosphatases (PP2Cs), therefore resulting in some CIPK26 becoming phosphorylated and hence activated. To resolve this, transgenic Arabidopsis plants that can be induced to express CIPK26 could be exposed to ABA or a solvent control prior to undergoing mass spectrometry analysis.

Seedlings overexpressing a constitutively active version of CIPK26 display increased sensitivity to ABA when compared to seedlings overexpressing the unmodified form of CIPK26 (Fig. 9). This finding is in agreement with the previous finding that plants overexpressing CIPK26 are hypersensitive to ABA, as a stabilized form of CIPK26 would be expected to exaggerate seedling sensitivity to ABA (Lyzenga et al., 2013). This is because the active kinase is capable of constitutively acting on ABA-responsive transcription factors such as ABI5. As a result, these transcription factors promote transcription of stress response genes, thereby resulting in an exaggerated ABA response in seedlings.

4.2.1 CIPK26 and KEG Phosphorylation and Ubiquitination

Regulation of cellular signaling elements, such as kinases, by a combination of phosphorylation and ubiquitination has been observed for some time (Hunter, 2007). Phosphorylation, dephosphorylation and ubiquitination are all implicated in ABA signaling (Mitula et al, 2015; Ding et al., 2015). More recently the variety of cellular targets that can be phosphorylated and ubiquitinated has come to light, this includes not only kinases, but also E3 ligases and targets of E3 ligases. Counter-regulation of post-translational modifications, where one modification opposes the typical action of another, is becoming increasingly evident in the literature (Hunter, 2007).

Phosphorylation affects the stability and activity of E3 ligase substrates. The inactivation of CIPK26 is attained through dephosphorylation by two clade A type 2 C protein phosphatases (PP2Cs), ABI1 and ABI2, implicated in the negative regulation of ABA signaling (Lyzenga et al., 2013; Weissman et al., 2011; Park et al., 2009). CIPK26 is thought to be downregulated by KEG mediated ubiquitination and proteasomal

degradation when in an inactive state. This contrasts with the downregulation and degradation of many other activated kinases directly via ubiquitination and the 26S proteasome (Lu and Hunter, 2009).

Phosphorylation regulates the activity of E3 ubiquitin ligases through a variety of means. Phosphorylation negatively regulates KEG by stimulating the E3 to self-ubiquitinate in the presence of ABA, targeting it for proteasome dependent degradation (Liu & Stone, 2010). A kinase inhibitor prevents this ABA-induced KEG degradation, while phosphorylated KEG displays increased self-ubiquitination activity (Liu & Stone, 2010). Phosphorylation is therefore heavily tied to KEGs E3 ligase activities. This work adds an additional element of complexity to KEG regulation by proposing that active CIPK26 phosphorylates KEG to promote KEG degradation. The phosphorylation of a RING-type E3 ubiquitin ligase by a member of the group of SNF1-related kinases has been previously documented (Ding et al., 2015). It was recently demonstrated that the RING-type E3 CHYR1, which is implicated in ABA and drought responses, interacts with SnRK2 protein kinases and can be phosphorylated by SnRK2.6 to modulate its function (Ding et al., 2015). Therefore, the phosphorylation of E3 ubiquitin ligases by SNF1- related kinases may be a relatively common mechanism used to regulate E3 ligase activity.

4.2.2 A Model of CIPK26 and KEG Reciprocal Regulation

This work, in combination with previous findings on the relationship between KEG and CIPK26, culminates in a model wherein low ABA conditions, or the absence of a stimulus like stress, KEG and the clade A PP2Cs ABI1 and ABI2 act to keep CIPK26 inactive (Lyzenga et al., 2013; Lee et al., 2007). ABA-responsive transcription factors are

also inactive in low ABA conditions and are targeted for degradation by the 26S proteasome. In the presence of ABA, or in response to stress, activated CIPK26 is stable and phosphorylates KEG, promoting KEG self-ubiquitination and degradation (Fig. 17). This model links KEG activity and the perception of ABA, as CIPK26 is known to interact with core ABA signaling network elements (Lyzenga et al., 2013; Weiner et al, 2010).

Figure 17. Model of KEG and CIPK26 reciprocal regulation. a) In the absence of ABA and stress, KEG negatively regulates the ABA signalling pathway; KEG ubiquitinates CIPK26 and the kinase is degraded by the 26S proteasome. b) In the presence of ABA, in periods of stress, CIPK26 is active and stable and phosphorylates KEG, which promotes KEG self-inhibition. KEG self-ubiquitinates and is subsequently degraded by the 26S proteasome. This model further links KEG activity to ABA signaling, and ABA perception in particular, as CIPK26 interacts with core elements of the ABA signaling network. This model also demonstrates how CIPK26 and KEG can each act to regulate the activity of the other, depending on surrounding conditions.

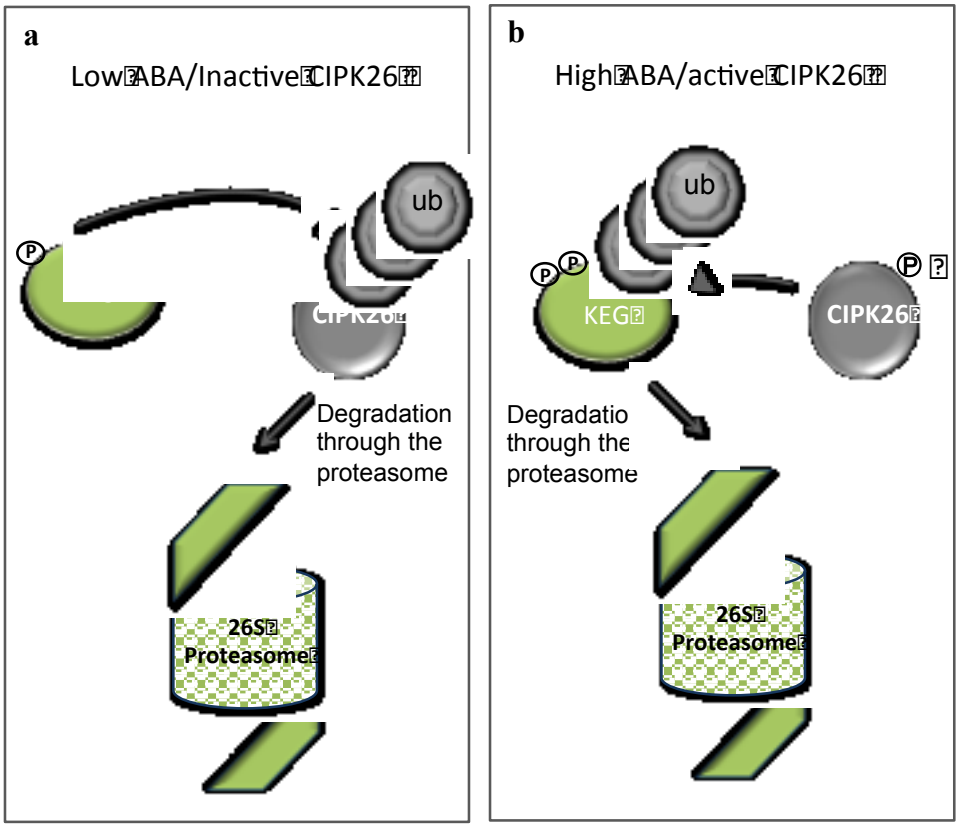
a
Low ABA/Inactive CIPK26
ub
P
Degradation through the proteasome
26S Proteasome
b
High ABA/active CIPK26
ub
P
P
KEG
CIPK26
P
Degradatio through the proteasome
26S Proteasome

4.3 Conclusions

Here, a novel substrate of the RING-type E3 ligase XBAT32, NDL1, was identified and the relationship between the RING-type E3 ligase KEG and one of its substrates, CIPK26, was further characterized. The work contributes to a growing body of knowledge on how the ubiquitin proteasome system, E3 ligases, and targets of E3 ligases, mediate and respond to hormone signaling. This work provides additional support for the involvement of the UPS in the regulation of major hormone signaling pathways implicated in stress, growth and development in plants. The regulation of NDL1 by XBAT32, an E3 ligase implicated in ethylene biosynthesis, may serve essential roles during development in the establishment of auxin gradients and the formation of lateral roots. Auxin regulation is fundamental to lateral root development, which is critical for plant survival. Meanwhile, the counter-regulatory action of CIPK26 on KEG in response to ABA likely serves vital functions in plant responses to external stress, as the resulting degradation of KEG allows for the activation of stress response genes by ABA-responsive transcription factors. Abiotic stress is now considered the single most harmful factor affecting the growth and productivity of crops around the world (Gao et al., 2007). The findings herein contribute to our understanding of essential processes in *Arabidopsis thaliana* and could enable the future development of plants that grow under adverse environmental conditions. This is an important area for future work, now more than ever, considering the major effects of climate change on crop viability and the health of soil.

REFERENCES

Abràmoff, M. D., Magalhães, P. J., & Ram, S. J. (2004). Image processing with ImageJ. *Biophotonics International*, *11*(7), 36-42.

Ardley, H. C., & Robinson, P. A. (2005). E3 ubiquitin ligases. *Essays in Biochemistry*, *41*, 15-30.

Behrends, C., & Harper, J. W. (2011). Constructing and decoding unconventional ubiquitin chains. *Nature Structural & Molecular Biology*, *18*(5), 520-528.

Bhattacharyya, S., Yu, H., Mim, C., & Matouschek, A. (2014). Regulated protein turnover: snapshots of the proteasome in action. *Nature Reviews Molecular Cell Biology*, *15*(2), 122-133.

Book, A. J., Gladman, N. P., Lee, S. S., Scalf, M., Smith, L. M., & Vierstra, R. D. (2010). Affinity purification of the Arabidopsis 26 S proteasome reveals a diverse array of plant proteolytic complexes. *Journal of Biological Chemistry*, *285*(33), 25554-25569.

Borden, K. L. (2000). RING domains: master builders of molecular scaffolds? *Journal of Molecular Biology*, *295*(5), 1103-1112.

Bremm, A., Freund, S. M., & Komander, D. (2010). Lys11-linked ubiquitin chains adopt compact conformations and are preferentially hydrolyzed by the deubiquitinase Cezanne. *Nature Structural & Molecular Biology*, *17*(8), 939-947.

Callis, J. (2014). The ubiquitination machinery of the ubiquitin system. *The Arabidopsis Book*, e0174.

Casimiro, I., Marchant, A., Bhalerao, R. P., Beeckman, T., Dhooge, S., Swarup, R., ... & Bennett, M. (2001). Auxin transport promotes Arabidopsis lateral root initiation. *The Plant Cell*, *13*(4), 843-852.

Chaves-Sanjuan, A., Sanchez-Barrena, M. J., Gonzalez-Rubio, J. M., Moreno, M., Ragel, P., Jimenez, M., ... & Albert, A. (2014). Structural basis of the regulatory mechanism of the plant CIPK family of protein kinases controlling ion homeostasis and abiotic stress. *Proceedings of the National Academy of Sciences of the USA*, *111*(42), E4532-E4541.

Chen, X., Qiu, J. D., Shi, S. P., Suo, S. B., Huang, S. Y., & Liang, R. P. (2013). Incorporating key position and amino acid residue features to identify general and species-specific Ubiquitin conjugation sites. *Bioinformatics*, *29*(13), 1614-1622.

Chen, Y. T., Liu, H., Stone, S., & Callis, J. (2013). ABA and the ubiquitin E3 ligase KEEP ON GOING affect proteolysis of the Arabidopsis thaliana transcription factors ABF1 and ABF3. *The Plant Journal*, *75*(6), 965-976.

Ciechanover, A., Heller, H., Elias, S., Haas, A. L., & Hershko, A. (1980). ATP-dependent conjugation of reticulocyte proteins with the polypeptide required for protein degradation. *Proceedings of the National Academy of Sciences of the USA*, *77*(3), 1365-1368.

Clough, S. J., & Bent, A. F. (1998). Floral dip: a simplified method for Agrobacterium - mediated transformation ofArabidopsis thaliana. *The Plant Journal*, *16*(6), 735-743.

Craig, A., Ewan, R., Mesmar, J., Gudipati, V., & Sadanandom, A. (2009). E3 ubiquitin ligases and plant innate immunity. *Journal of Experimental Botany*, *60*(4), 1123-1132.

De Bie, P., & Ciechanover, A. (2011). Ubiquitination of E3 ligases: self-regulation of the ubiquitin system via proteolytic and non-proteolytic mechanisms. *Cell Death & Differentiation*, *18*(9), 1393-1402.

De Smet, I., Tetsumura, T., De Rybel, B., dit Frey, N. F., Laplaze, L., Casimiro, I., ... & Inzé, D. (2007). Auxin-dependent regulation of lateral root positioning in the basal meristem of Arabidopsis. *Development*, *134*(4), 681-690.

Dikic, I., Wakatsuki, S., & Walters, K. J. (2009). Ubiquitin-binding domains—from structures to functions. *Nature Reviews Molecular Cell Biology*, *10*(10), 659-671.

Ding, S., Zhang, B., & Qin, F. (2015). Arabidopsis RZFP34/CHYR1, a ubiquitin E3 ligase, regulates stomatal movement and drought tolerance via SnRK2. 6-mediated phosphorylation. *The Plant Cell*, *27*(11), 3228-3244.

Dubrovsky, J. G., Sauer, M., Napsucialy-Mendivil, S., Ivanchenko, M. G., Friml, J., Shishkova, S., ... & Benková, E. (2008). Auxin acts as a local morphogenetic trigger to specify lateral root founder cells. *Proceedings of the National Academy of Sciences of the USA*, *105*(25), 8790-8794.

Earley, K. W., Haag, J. R., Pontes, O., Opper, K., Juehne, T., Song, K., & Pikaard, C. S. (2006). Gateway-compatible vectors for plant functional genomics and proteomics. *The Plant Journal*, *45*(4), 616-629.

Eletr, Z. M., & Wilkinson, K. D. (2014). Regulation of proteolysis by human deubiquitinating enzymes. *Biochimica et Biophysica Acta (BBA)-Molecular Cell Research*, *1843*(1), 114-128.

Fernando, V. D., & Schroeder, D. F. (2016). Role of ABA in Arabidopsis Salt, Drought, and Desiccation Tolerance. In A. K. Shanker & C. Shanker (Eds.), *Abiotic and Biotic Stress in Plants – Recent Advances and Future Perspectives* (pp. 507-524). InTech.

Finkelstein, R. (2013). Abscisic acid synthesis and response. *The Arabidopsis Book*, 11(e0166).

Finley, D. (2009). Recognition and processing of ubiquitin-protein conjugates by the proteasome. *Annual Review of Biochemistry*, *78*, 477.

Flick, K., Raasi, S., Zhang, H., Yen, J. L., & Kaiser, P. (2006). A ubiquitin-interacting motif protects polyubiquitinated Met4 from degradation by the 26S proteasome. *Nature Cell Biology*, *8*(5), 509-515.

Freemont, P. S. (1993). The RING finger. *Annals of the New York Academy of Sciences*, *684*(1), 174-192.

Fu, H., Lin, Y. L., & Fatimababy, A. S. (2010). Proteasomal recognition of ubiquitylated substrates. *Trends in Plant Science*, *15*(7), 375-386.

Gao, J. P., Chao, D. Y., & Lin, H. X. (2007). Understanding abiotic stress tolerance mechanisms: recent studies on stress response in rice. *Journal of Integrative Plant Biology*, *49*(6), 742-750.

Garcia-Gonzalo, F. R., & Rosa, J. L. (2005). The HERC proteins: functional and evolutionary insights. *Cellular and Molecular Life Sciences CMLS*, *62*(16), 1826-1838.

Glickman, M. H., & Ciechanover, A. (2002). The ubiquitin-proteasome proteolytic pathway: destruction for the sake of construction. *Physiological Reviews*, *82*(2), 373- 428.

Gong, D., Gong, Z., Guo, Y., Chen, X., & Zhu, J.K. (2002. a). Biochemical and functional characterization of PKS11, a novel Arabidopsis protein kinase. *The Journal of Biological Chemistry*, 277, 28340-28350.

Gong, D., Zhang, C., Chen, X., Gong, Z., & Zhu, J.K. (2002. b). Constitutive activation and transgenic evaluation of the function of an arabidopsis PKS protein kinase. *The Journal of Biological Chemistry*, 277, 42088-42096.

Grabbe, C., & Dikic, I. (2009). Functional roles of ubiquitin-like domain (ULD) and ubiquitin-binding domain (UBD) containing proteins. *Chemical Reviews*, *109*(4), 1481-1494.

Groll, M., Ditzel, L., Löwe, J., Stock, D., Bochtler, M., Bartunik, H. D., & Huber, R. (1997). Structure of 20S proteasome from yeast at 2.4Å resolution. *Nature*, 386(6624), 463-471.

Gu, Y., & Innes, R. W. (2012). The KEEP ON GOING protein of Arabidopsis regulates intracellular protein trafficking and is degraded during fungal infection. *The Plant Cell*, *24*(11), 4717-4730.

Haglund, K., Di Fiore, P. P., & Dikic, I. (2003). Distinct monoubiquitin signals in receptor endocytosis. *Trends in Biochemical Sciences*, *28*(11), 598-604.

Hashimoto, K., Eckert, C., Anschütz, U., Scholz, M., Held, K., Waadt, R., ... & Kudla, J. (2012). Phosphorylation of calcineurin B-like (CBL) calcium sensor proteins by their CBL-interacting protein kinases (CIPKs) is required for full activity of CBL-CIPK complexes toward their target proteins. *Journal of Biological Chemistry*, *287*(11), 7956-7968.

Hicke, L. (2001). Protein regulation by monoubiquitin. *Nature Reviews Molecular Cell Biology*, *2*(3), 195-201.

Himmelbach, A., Yang, Y., & Grill, E. (2003). Relay and control of abscisic acid signaling. *Current Opinion in Plant Biology*, *6*(5), 470-479.

Hrabak, E. M., Chan, C. W., Gribskov, M., Harper, J. F., Choi, J. H., Halford, N., ... & Thomas, M. (2003). The Arabidopsis CDPK-SnRK superfamily of protein kinases. *Plant Physiology*, *132*(2), 666-680.

Hua, Z., & Vierstra, R. D. (2011). The cullin-RING ubiquitin-protein ligases. *Annual Review of Plant Biology*, *62*, 299-334.

Huibregtse, J. M., Scheffner, M., Beaudenon, S., & Howley, P. M. (1995). A family of proteins structurally and functionally related to the E6-AP ubiquitin-protein ligase. *Proceedings of the National Academy of Sciences of the USA*, *92*(7), 2563-2567.

Hunter, T. (2007). The age of crosstalk: phosphorylation, ubiquitination, and beyond. *Molecular Cell*, *28*(5), 730-738.

Jentsch, S., & Pyrowolakis, G. (2000). Ubiquitin and its kin: how close are the family ties?. *Trends in Cell Biology*, *10*(8), 335-342.

Khatri, N., & Mudgil, Y. (2015). Hypothesis: NDL proteins function in stress responses by regulating microtubule organization. *Frontiers in Plant Science*, *6(947)*.

Kim, W., Bennett, E. J., Huttlin, E. L., Guo, A., Li, J., Possemato, A., ... & Harper, J. W. (2011). Systematic and quantitative assessment of the ubiquitin-modified proteome. *Molecular Cell*, *44*(2), 325-340.

Kisselev, A. F., & Goldberg, A. L. (2001). Proteasome inhibitors: from research tools to drug candidates. *Chemistry & Biology*, *8*(8), 739-758.

Kisselev, A. F., Akopian, T. N., Castillo, V., & Goldberg, A. L. (1999). Proteasome active sites allosterically regulate each other, suggesting a cyclical bite-chew mechanism for protein breakdown. *Molecular Cell*, *4*(3), 395-402.

Klopffleisch, K., Phan, N., Augustin, K., Bayne, R. S., Booker, K. S., Botella, J. R., ... & Jones, A. M. (2011). Arabidopsis G-protein interactome reveals connections to cell wall carbohydrates and morphogenesis. *Molecular Systems Biology*, *7*(1), 532.

Komander, D., & Rape, M. (2012). The ubiquitin code. *Annual Review of Biochemistry*, *81*, 203-229.

Kong, L., Cheng, J., Zhu, Y., Ding, Y., Meng, J., Chen, Z., ... & Gong, Z. (2015). Degradation of the ABA co-receptor ABI1 by PUB12/13 U-box E3 ligases. *Nature Communications*, *6(8630)*.

Kraft, E., Stone, S. L., Ma, L., Su, N., Gao, Y., Lau, O. S., ... & Callis, J. (2005). Genome analysis and functional characterization of the E2 and RING-type E3 ligase ubiquitination enzymes of Arabidopsis. *Plant Physiology*, *139*(4), 1597-1611.

Kräuter-Canham, R., Bronner, R., Evrard, J. L., Hahne, G., Friedt, W., & Steinmetz, A. (1997). A transmitting tissue-and pollen-expressed protein from sunflower with sequence similarity to the human RTP protein. *Plant Science*, *129*(2), 191-202.

Kuroda, H., Takahashi, N., Shimada, H., Seki, M., Shinozaki, K., & Matsui, M. (2002). Classification and expression analysis of Arabidopsis F-box-containing protein genes. *Plant and Cell Physiology*, *43*(10), 1073-1085.

Lan, W. Z., Lee, S. C., Che, Y. F., Jiang, Y. Q., & Luan, S. (2011). Mechanistic analysis of AKT1 regulation by the CBL–CIPK–PP2CA interactions. *Molecular Plant*, *4*(3), 527-536.

Lazarescu, E., Friedt, W., Horn, R., & Steinmetz, A. (2006). Expression analysis of the sunflower SF21 gene family reveals multiple alternative and organ-specific splicing of transcripts. *Gene*, *374*, 77-86.

Lecker, S. H., Goldberg, A. L., & Mitch, W. E. (2006). Protein degradation by the ubiquitin–proteasome pathway in normal and disease states. *Journal of the American Society of Nephrology*, *17*(7), 1807-1819.

Lee, J. E., & Kim, J. H. (2015). SUMO modification regulates the protein stability of NDRG1. *Biochemical and Biophysical Research Communications*, *459*(1), 161-165.

Lee, S. C., Lan, W. Z., Kim, B. G., Li, L., Cheong, Y. H., Pandey, G. K., ... & Luan, S. (2007). A protein phosphorylation/dephosphorylation network regulates a plant potassium channel. *Proceedings of the National Academy of Sciences of the USA*, *104*(40), 15959-15964.

Lewis, D. R., Negi, S., Sukumar, P., & Muday, G. K. (2011). Ethylene inhibits lateral root development, increases IAA transport and expression of PIN3 and PIN7 auxin efflux carriers. *Development*, *138*(16), 3485-3495.

Li, A., Gao, X., Ren, J., Jin, C., & Xue, Y. (2009). BDM-PUB: computational prediction of protein ubiquitination sites with a Bayesian discriminant method. *BDM-PUB: Computational Prediction of Protein Ubiquitination Sites with a Bayesian Discriminant Method*.

Li, W., & Ye, Y. (2008). Polyubiquitin chains: functions, structures, and mechanisms. *Cellular and Molecular Life Sciences*, *65*(15), 2397-2406.

Liu, H., & Stone, S. L. (2010). Abscisic acid increases Arabidopsis ABI5 transcription factor levels by promoting KEG E3 ligase self-ubiquitination and proteasomal degradation. *The Plant Cell*, *22*(8), 2630-2641.

Liu, H., & Stone, S. L. (2013). Cytoplasmic degradation of the Arabidopsis transcription factor abscisic acid insensitive 5 is mediated by the RING-type E3 ligase KEEP ON GOING. *Journal of Biological Chemistry*, *288*(28), 20267-20279.

Liu, H., & Stone, S. L. (2014). Regulation of ABI5 turnover by reversible post-translational modifications. *Plant Signaling & Behavior*, *9*(1), e27577.

Liu, Y. C., Penninger, J., & Karin, M. (2005). Immunity by ubiquitylation: a reversible process of modification. *Nature Reviews Immunology*, *5*(12), 941-952.

Lopez-Molina, L., Mongrand, S., & Chua, N. H. (2001). A postgermination developmental arrest checkpoint is mediated by abscisic acid and requires the ABI5 transcription factor in Arabidopsis. *Proceedings of the National Academy of Sciences of the USA*, *98*(8), 4782-4787.

Lorick, K. L., Jensen, J. P., Fang, S., Ong, A. M., Hatakeyama, S., & Weissman, A. M. (1999). RING fingers mediate ubiquitin-conjugating enzyme (E2)-dependent ubiquitination. *Proceedings of the National Academy of Sciences of the USA*, *96*(20), 11364-11369.

Lowe, J., Stock, D., Jap, B., Zwickl, P., Baumeister, W., & Huber, R. (1995). Crystal structure of the 20S proteasome from the archaeon T. acidophilum at 3.4 A resolution. *Science*, *268*(5210), 533-539.

Ludwikow, A. (2015). Targeting proteins for proteasomal degradation-a new function of Arabidopsis ABl1 protein phosphatase 2C. *Frontiers in Plant Science*, 6, 310.

Lyzenga, W. J., & Stone, S. L. (2012). Abiotic stress tolerance mediated by protein ubiquitination. *Journal of Experimental Botany*, 63(2), 599-616.

Lyzenga, W. J., & Stone, S. L. (2012). Regulation of ethylene biosynthesis through protein degradation. *Plant Signaling & Behavior*, *7*(11), 1438-1442.

Lyzenga, W. J., Booth, J. K., & Stone, S. L. (2012). The Arabidopsis RING-type E3 ligase XBAT32 mediates the proteasomal degradation of the ethylene biosynthetic enzyme, 1-aminocyclopropane-1-carboxylate synthase 7. *The Plant Journal*, *71*(1), 23-34.

Lyzenga, W. J., Liu, H., Schofield, A., Muise-Hennessey, A., & Stone, S. L. (2013). Arabidopsis CIPK26 interacts with KEG, components of the ABA signalling network and is degraded by the ubiquitin–proteasome system. *Journal of Experimental Botany*, *64*(10), 2779-2791.

Malamy, J. E., & Benfey, P. N. (1997). Organization and cell differentiation in lateral roots of Arabidopsis thaliana. *Development*, *124*(1), 33-44.

Mazzucotelli, E., Belloni, S., Marone, D., De Leonardis, A. M., Guerra, D., Di Fonzo, N., ... & Mastrangelo, A. M. (2006). The E3 ubiquitin ligase gene family in plants: regulation by degradation. *Current Genomics*, *7*(8), 509-522.

McVey, S. (2015). Role of Arabidopsis thaliana RING-Type E3 Ligase XBAT35.2 in Regulating ACD11 Stability (masters thesis-AMICUS No. 44379504). Dalhousie University, Halifax, Nova Scotia.

Mitula, F., Tajdel, M., Cieśla, A., Kasprowicz-Maluśki, A., Kulik, A., Babula-Skowrońska, D., ... & Ludwików, A. (2015). Arabidopsis ABA-Activated Kinase MAPKKK18 is Regulated by Protein Phosphatase 2C ABI1 and the Ubiquitin–Proteasome Pathway. *Plant and Cell Physiology*, pcv146.

Mudgil, Y., Ghawana, S., & Jones, A. M. (2013). N-MYC DOWN-REGULATED-LIKE proteins regulate meristem initiation by modulating auxin transport and MAX2 expression. *PloS One*, *8*(11), e77863.

Mudgil, Y., Uhrig, J. F., Zhou, J., Temple, B., Jiang, K., & Jones, A. M. (2009). Arabidopsis N-MYC DOWNREGULATED-LIKE1, a positive regulator of auxin transport in a G protein–mediated pathway. *The Plant Cell*, *21*(11), 3591-3609.

Mukhopadhyay, D., & Riezman, H. (2007). Proteasome-independent functions of ubiquitin in endocytosis and signaling. *Science*, *315*(5809), 201-205.

Nakasone, M. A., Livnat-Levanon, N., Glickman, M. H., Cohen, R. E., & Fushman, D. (2013). Mixed-linkage ubiquitin chains send mixed messages. *Structure*, *21*(5), 727-740.

Negi, S., Ivanchenko, M. G., & Muday, G. K. (2008). Ethylene regulates lateral root formation and auxin transport in Arabidopsis thaliana. *The Plant Journal*, *55*(2), 175-187.

Nodzon, L. A., Xu, W. H., Wang, Y., Pi, L. Y., Chakrabarty, P. K., & Song, W. Y. (2004). The ubiquitin ligase XBAT32 regulates lateral root development in Arabidopsis. *The Plant Journal*, *40*(6), 996-1006.

Nussbaum, A. K., Dick, T. P., Keilholz, W., Schirle, M., Stevanović, S., Dietz, K., ... & Rammensee, H. G. (1998). Cleavage motifs of the yeast 20S proteasome β subunits deduced from digests of enolase 1. *Proceedings of the National Academy of Sciences of the USA*, *95*(21), 12504-12509.

Ohta, M., Guo, Y., Halfter, U., & Zhu, J. K. (2003). A novel domain in the protein kinase SOS2 mediates interaction with the protein phosphatase 2C ABI2. *Proceedings of the National Academy of Sciences of the USA*, *100*(20), 11771-11776.

Park, S. Y., Fung, P., Nishimura, N., Jensen, D. R., Fujii, H., Zhao, Y., ... & Alfred, S. E. (2009). Abscisic acid inhibits type 2C protein phosphatases via the PYR/PYL family of START proteins. *Science*, *324*(5930), 1068-1071.

Park, S., Tian, G., Roelofs, J., & Finley, D. (2010). Assembly manual for the proteasome regulatory particle: the first draft. *Biochemical Society Transactions*, *38*(1), 6-13.

Passmore, L. A., & Barford, D. (2004). Getting into position: the catalytic mechanisms of protein ubiquitylation. *Biochemical Journal*, *379*(3), 513-525.

Pauwels, L., Ritter, A., Goossens, J., Durand, A. N., Liu, H., Gu, Y., ... & Van Leene, J. (2015). The RING E3 Ligase KEEP ON GOING Modulates JASMONATE ZIM-DOMAIN12 Stability. *Plant Physiology*, *169*(2), 1405-1417.

Péret, B., De Rybel, B., Casimiro, I., Benková, E., Swarup, R., Laplaze, L., ... & Bennett, M. J. (2009). Arabidopsis lateral root development: an emerging story. *Trends in Plant Science*, *14*(7), 399-408.

Pickart, C. M. (2001). Mechanisms underlying ubiquitination. *Annual Review of Biochemistry*, *70*(1), 503-533.

Prasad, M. E., Schofield, A., Lyzenga, W., Liu, H., & Stone, S. L. (2010). Arabidopsis RING E3 ligase XBAT32 regulates lateral root production through its role in ethylene biosynthesis. *Plant Physiology*, *153*(4), 1587-1596.

Risseeuw, E. P., Daskalchuk, T. E., Banks, T. W., Liu, E., Cotelesage, J., Hellmann, H., ... & Crosby, W. L. (2003). Protein interaction analysis of SCF ubiquitin E3 ligase subunits from Arabidopsis. *The Plant Journal*, *34*(6), 753-767.

Sakiyama-Sogo, M., & Shibaoka, H. (1993). Gibberellin A3 and abscisic acid cause the reorientation of cortical microtubules in epicotyl cells of the decapitated dwarf pea. *Plant and Cell Physiology*, *34*(3), 431-437.

Santos, F., Teale, W., Fleck, C., Volpers, M., Ruperti, B., & Palme, K. (2010). Modelling polar auxin transport in developmental patterning. *Plant Biology*, *12*(s1), 3-14.

Sanyal, S. K., Pandey, A., & Pandey, G. K. (2015). The CBL–CIPK signaling module in plants: a mechanistic perspective. *Physiologia Plantarum*, *155*(2), 89-108.

Schechtman, D., Mochly-Rosen, D., & Ron, D. (2003). Glutathione S-transferase pull-down assay. *Protein Kinase C Protocols*, 345-350.

Sedgwick, S. G., & Smerdon, S. J. (1999). The ankyrin repeat: a diversity of interactions on a common structural framework. *Trends in Biochemical Sciences*, *24*(8), 311-316.

Seki, M., Ishida, J., Narusaka, M., Fujita, M., Nanjo, T., Umezawa, T., ... & Satou, M. (2002). Monitoring the expression pattern of around 7,000 Arabidopsis genes under ABA treatments using a full-length cDNA microarray. *Functional & Integrative genomics*, *2*(6), 282-291.

Shibaoka, H. (1994). Plant hormone-induced changes in the orientation of cortical microtubules: alterations in the cross-linking between microtubules and the plasma membrane. *Annual Review of Plant Biology*, *45*(1), 527-544.

Smalle, J., & Vierstra, R. D. (2004). The ubiquitin 26S proteasome proteolytic pathway. *Annual Review of Plant Biology*, *55*, 555-590.

Stone, S. (2014). The role of ubiquitin and the 26S proteasome in plant abiotic stress signalling. *Frontiers in Plant Science*, 5(135), 1-10.

Stone, S. L., & Callis, J. (2007). Ubiquitin ligases mediate growth and development by promoting protein death. *Current Opinion in Plant Biology*,*10*(6), 624-632.

Stone, S. L., Hauksdóttir, H., Troy, A., Herschleb, J., Kraft, E., & Callis, J. (2005). Functional analysis of the RING-type ubiquitin ligase family of Arabidopsis. *Plant Physiology*, *137*(1), 13-30.

Stone, S. L., Williams, L. A., Farmer, L. M., Vierstra, R. D., & Callis, J. (2006). KEEP ON GOING, a RING E3 ligase essential for Arabidopsis growth and development, is involved in abscisic acid signaling. *The Plant Cell*, *18*(12), 3415-3428.

Sun, L., & Chen, Z. J. (2004). The novel functions of ubiquitination in signaling. *Current Opinion in Cell Biology*, *16*(2), 119-126.

Thrower, J. S., Hoffman, L., Rechsteiner, M., & Pickart, C. M. (2000). Recognition of the polyubiquitin proteolytic signal. *The EMBO journal*, *19*(1), 94-102.

Turcu, F. E. R., Ventii, K. H., & Wilkinson, K. D. (2009). Regulation and cellular roles of ubiquitin-specific deubiquitinating enzymes. *Annual Review of Biochemistry*, *78*, 363.

Unverdorben, P., Beck, F., Śledź, P., Schweitzer, A., Pfeifer, G., Plitzko, J. M., ... & Förster, F. (2014). Deep classification of a large cryo-EM dataset defines the conformational landscape of the 26S proteasome. *Proceedings of the National Academy of Sciences of the USA*, *111*(15), 5544-5549.

Van Nocker, S., Deveraux, Q., Rechsteiner, M., & Vierstra, R. D. (1996). Arabidopsis MBP1 gene encodes a conserved ubiquitin recognition component of the 26S proteasome. *Proceedings of the National Academy of Sciences of the USA*, *93*(2), 856-860.

Verdecia, M. A., Joazeiro, C. A., Wells, N. J., Ferrer, J. L., Bowman, M. E., Hunter, T., & Noel, J. P. (2003). Conformational flexibility underlies ubiquitin ligation mediated by the WWP1 HECT domain E3 ligase. *Molecular Cell*, *11*(1), 249-259.

Verma, R., Aravind, L., Oania, R., McDonald, W. H., Yates, J. R., Koonin, E. V., & Deshaies, R. J. (2002). Role of Rpn11 metalloprotease in deubiquitination and degradation by the 26S proteasome. *Science*, *298*(5593), 611-615.

Vierstra, R. D. (2009). The ubiquitin–26S proteasome system at the nexus of plant biology. *Nature Reviews Molecular Cell Biology*, *10*(6), 385-397.

Voges, D., Zwickl, P., & Baumeister, W. (1999). The 26S proteasome: a molecular machine designed for controlled proteolysis. *Annual Review of Biochemistry*, *68*(1), 1015-1068.

Wang, K. L. C., Li, H., & Ecker, J. R. (2002). Ethylene biosynthesis and signaling networks. *The Plant Cell*, *14*(suppl 1), S131-S151.

Wang, Y. S., Pi, L. Y., Chen, X., Chakrabarty, P. K., Jiang, J., De Leon, A. L., ... & Ronald, P. C. (2006). Rice XA21 binding protein 3 is a ubiquitin ligase required for full Xa21-mediated disease resistance. *The Plant Cell*, *18*(12), 3635-3646.

Weiner, J. J., Peterson, F. C., Volkman, B. F., & Cutler, S. R. (2010). Structural and functional insights into core ABA signaling. *Current Opinion in Plant Biology*, *13*(5), 495-502.

Weinl, S., & Kudla, J. (2009). The CBL-CIPK Ca2+-decoding signaling network: function and perspectives. *New Phytologist*, *184*(3), 517-528.

Weissman, A. M., Shabek, N., & Ciechanover, A. (2011). The predator becomes the prey: regulating the ubiquitin system by ubiquitylation and degradation. *Nature Reviews Molecular Cell Biology*, *12*(9), 605-620.

Wenzel, T., Eckerskorn, C., Lottspeich, F., & Baumeister, W. (1994). Existence of a molecular ruler in proteasomes suggested by analysis of degradation products. *FEBS Letters*, *349*(2), 205-209.

Wilkinson, K. D., Ventii, K. H., Friedrich, K. L., & Mullally, J. E. (2005). The ubiquitin signal: assembly, recognition and termination. *EMBO Reports*, *6*(9), 815-820.

Williamson, A., Banerjee, S., Zhu, X., Philipp, I., Iavarone, A. T., & Rape, M. (2011). Regulation of ubiquitin chain initiation to control the timing of substrate degradation. *Molecular Cell*, *42*(6), 744-757.

Yang, S. F., & Hoffman, N. E. (1984). Ethylene biosynthesis and its regulation in higher plants. *Annual Review of Plant Physiology*, *35*(1), 155-189.

Yao, T., & Cohen, R. E. (2002). A cryptic protease couples deubiquitination and degradation by the proteasome. *Nature*, *419*(6905), 403-407.

Yee, D., & Goring, D. R. (2009). The diversity of plant U-box E3 ubiquitin ligases: from upstream activators to downstream target substrates. *Journal of Experimental Botany*, ern369.

Yu, Q., An, L., & Li, W. (2014). The CBL–CIPK network mediates different signaling pathways in plants. *Plant cell reports*, *33*(2), 203-214.

Yuan, X., Zhang, S., Liu, S., Yu, M., Su, H., Shu, H., & Li, X. (2013). Global analysis of ankyrin repeat domain C3HC4-type RING finger gene family in plants. *PloS One*, *8*(3), e58003.

Zheng, N., Wang, P., Jeffrey, P. D., & Pavletich, N. P. (2000). Structure of a c-Cbl–UbcH7 complex: RING domain function in ubiquitin-protein ligases. *Cell*, *102*(4), 533-539.

Zhou, R. H., Kokame, K., Tsukamoto, Y., Yutani, C., Kato, H., & Miyata, T. (2001). Characterization of the human NDRG gene family: a newly identified member, NDRG4, is specifically expressed in brain and heart. *Genomics*, *73*(1), 86-97.

APPENDIX I: SUPPLEMENTARY FIGURES

Supplemental figures here include replicates, as well as work conducted in collaboration with others.

Supplemental Figure 1. CIPK26 is phosphorylated following ABA treatment. a) Immunoprecipitation of CIPK26 using anti-HA affinity beads. Western blot (WB) probed with anti-HA antibodies showing presence of immunoprecipitated CIPK26-YFP-HA and CIPK26^{KR}-YFP-HA proteins extracted from 6-day-old *35S:CIPK26-YFP-HA* and *35S:CIPK26^{KR}-YFP-HA Arabidopsis thaliana* seedlings treated with (+) or without (-) 100µM ABA for 30 minutes. Col-0, control, represents protein extracts from 6-day-old wild type *Arabidopsis thaliana* plants (Columbia ecotype). Protein extracts were incubated with anti-HA affinity beads for 3 h. Black arrowhead indicates CIPK26-YFP-HA. b) Immunoprobing of Western blots (WB) using anti-phosphoserine antibodies to detect immunoprecipitated CIPK26. CIPK26-YFP-HA and CIPK26^{KR}-YFP-HA were isolated from protein extracts of *35S:CIPK26-YFP-HA* and *35S:CIPK26^{KR}-YFP-HA* transgenic seedlings treated with (+) or without (-) 100µM ABA for 30 min, by incubation with anti-HA affinity beads. Black arrowhead indicates CIPK26-YFP-HA.

a

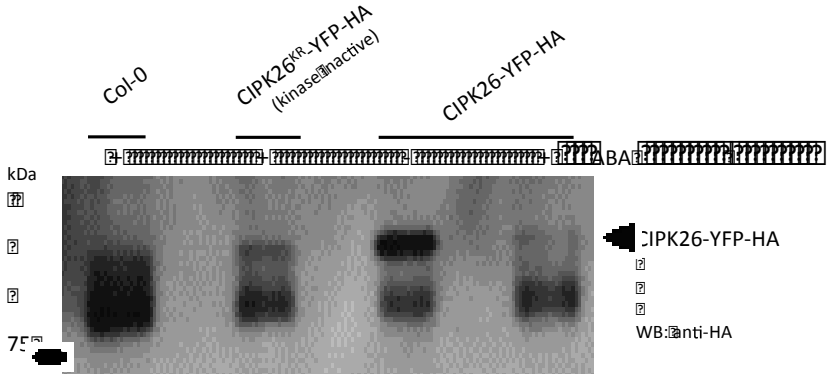
Col-0
CIPK26KR-YFP-HA
(kinase inactive)
CIPK26-YFP-HA
kDa
75
CIPK26-YFP-HA
WB: anti-HA

b

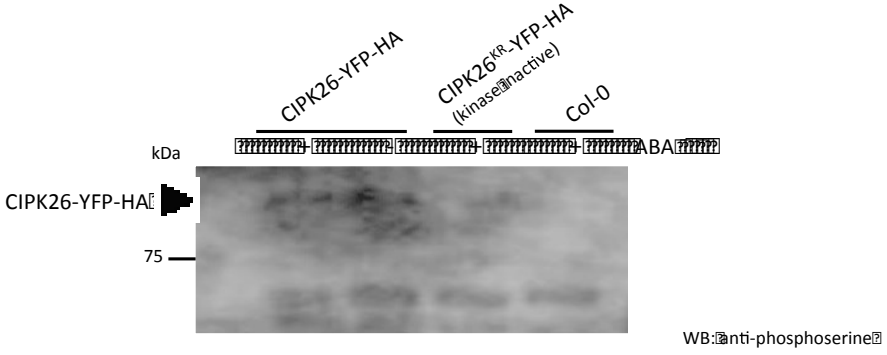
CIPK26-YFP-HA
CIPK26KR-YFP-HA
(kinase inactive)
Col-0
kDa
CIPK26-YFP-HA
75
WB: anti-phosphoserine

Supplemental Figure 2. Replicate of semi-*in vitro* ubiquitination assay. Purified recombinant His-Flag-NDL1 was used in semi-*in vitro* ubiquitination assays in combination with protein extract from wild type *Arabidopsis thaliana* seedlings. Numbers beneath blots indicate lanes. Purified His-Flag-NDL1 was detected by immunoprobing with anti-Flag antibodies and is represented in lane 1. In lane 3, this purified His-Flag-NDL1 was added to total Arabidopsis protein extracts and incubated with p62-agarose (ubiquitin-trap beads) for 4 h at 4 °C. In lane 2, purified His-Flag-NDL1 was not added to Arabidopsis protein extracts incubated with p62-agarose for 4 h at 4 °C. Probing of Western blots with anti-Flag antibodies revealed that p62-agarose isolated ubiquitin-modified His-Flag-NDL1 in lane 3. Col-0 is Columbia ecotype.

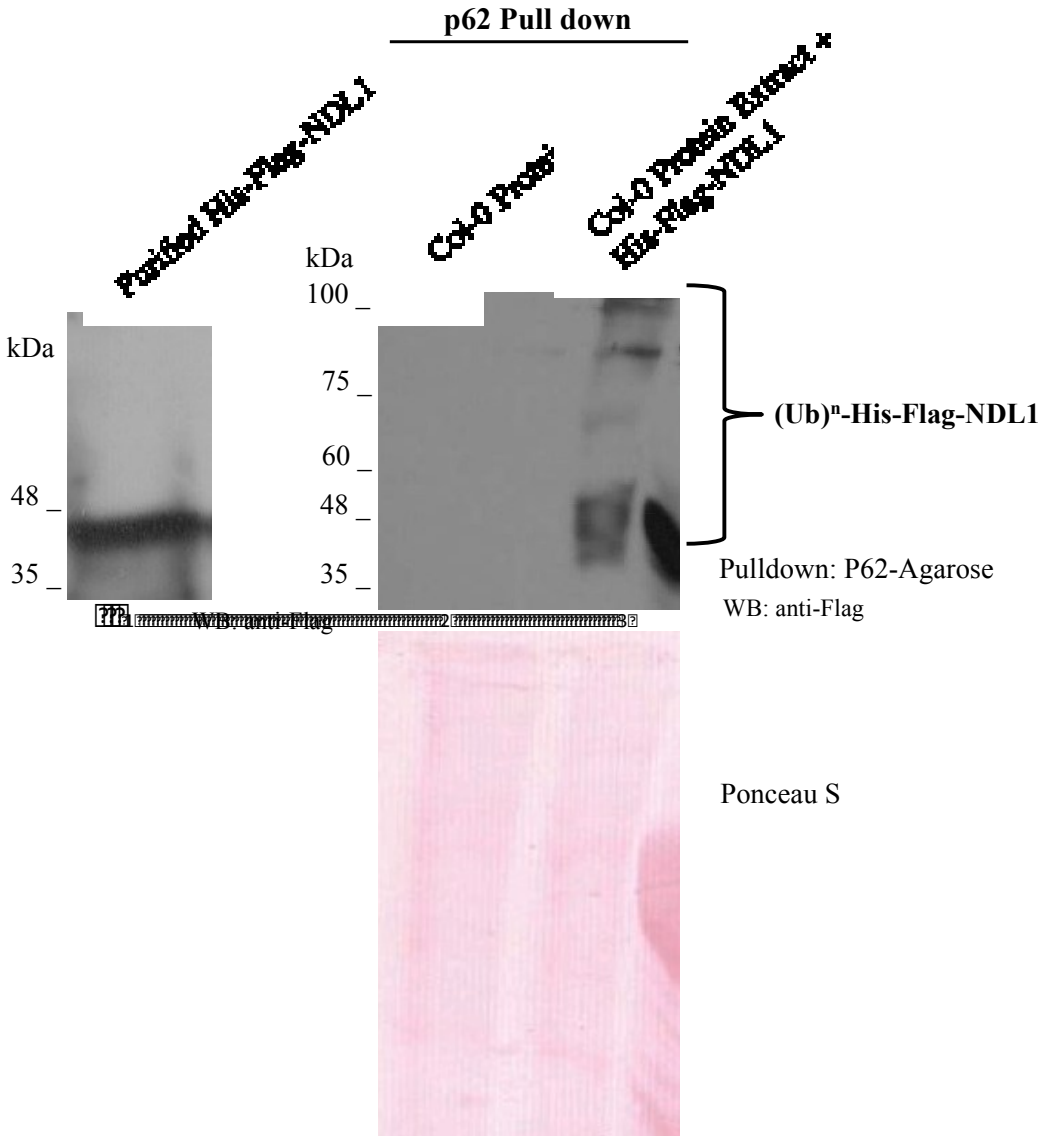
p62 Pull down
Purified His-Flag-NDL1
Cos-0 Protein
Cos-0 Protein Extract + His-Flag-NDL1
kDa
100
75
60
48
35
kDa
48
35
(Ub)n-His-Flag-NDL1
Pulldown: P62-Agarose
WB: anti-Flag
Ponceau S

Supplemental Figure 3. Repetition of the cell free degradation assay with wild type and *xbat32-1* plants and purified recombinant His-Flag-NDL1. Cell free degradation assays were performed with *Arabidopsis thaliana* protein extracts from wild type (wt) and *xbat32-1* plants, and purified His-Flag-NDL1. His-Flag-NDL1 was mixed with total protein extract with (+) or without (-) 50 μM of MG132. Amount of His-Flag-NDL1 remaining at each time point was determined by probing Western blots (WB) with anti-Flag antibodies. Apparent air bubble at 0 min time point in the wild type (-) MG132 sample. His-Flag-NDL1 appears more stable in the *xbat32-1* background, as compared to the wt background in the absence of a proteasome inhibitor.

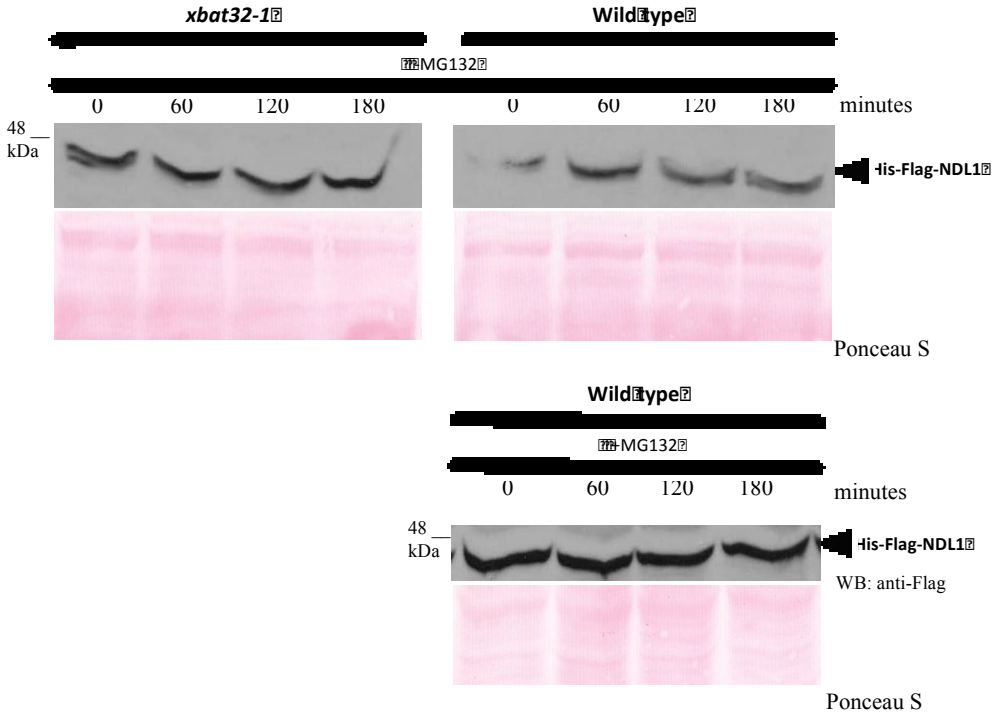
xbat32-1
Wild type
MG132
0
60
120
180
0
60
120
180
minutes
48
kDa
His-Flag-NDL1
Ponceau S
Wild type
MG132
0
60
120
180
minutes
48
kDa
His-Flag-NDL1
WB: anti-Flag
Ponceau S